SUPER DEEP GEOTHERMAL POTENTIAL IN THE OIL SANDS REGION OF ALBERTA

Presented by GLJ Ltd. to the Geothermal Working Group of COSIA

Reviewed By:
John Hirschmiller, P.Geo.
GLJ Ltd.

Darcy Riva, P.Eng.
GLJ Ltd.

December 22, 2022
S1223592

CANADA'S OIL SANDS INNOVATION ALLIANCE

December 21, 2022

Mr. Robert Mugo
COSIA GHG EPA Director
Canadian Oil Sands Innovation Alliance
520 5th Avenue SW
Suite 1700, Calgary, AB, T2P 3R7

SUPER DEEP GEOTHERMAL POTENTIAL
IN THE OIL SANDS REGION OF ALBERTA - 1223592

Regarding the Super Deep Geothermal Potential project, GLJ Ltd. (GLJ) is pleased to present its report for the understanding of super deep geothermal. The report focuses on a subsurface review of the geothermal potential, addresses drilling risks and facilities required and culminates in an economic comparison of super deep geothermal technology to conventional boilers for SAGD.

We trust the report is sufficient for your purposes. Should you have any questions regarding this repot, please contact the undersigned at 1-403-266-9423 or jhirschmiller@gljpc.com.

Yours truly,

John Hirschmiller, P. Geo. | GLJ Ltd | Senior Geologist, Geothermal Lead

Table of Contents

List of Figures

List of Tables

Certification of Qualifications

This report was prepared to the best of the knowledge of the authors. All data furnished in this report was prepared and reviewed by the authors. Data and interpretations presented in this report are of the opinion of the authors and are believed accurate in nature as a function of the quality and quantity of the available data. Estimates and interpretations presented herein are considered reasonable and should be accepted with the understanding that revisions may be justified if additional data is acquired.

John J. Hirschmiller, P.Geo.
Senior Geologist, Geothermal Lead

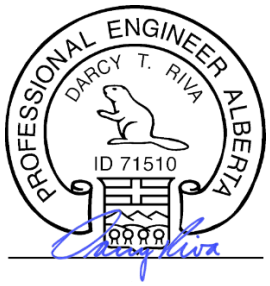

Darcy T. Riva, P.Eng.
Manager, Engineering

GLJ Ltd. Permit to Practice #2066
Association of Professional Engineers and Geoscientists of Alberta

ABOUT GLJ

GLJ was founded on 1976 with the mandate of providing quality engineering and geological services to the oil and gas industry, with a core focus on provision of independent reserves and resources assessments, evaluations, audits, and process reviews, most often utilized for corporate governance, year-end disclosure, and transactions.

As global energy consultants with over 50 years of experience, GLJ illuminates a better path forward. GLJ provides services for the implementation and evaluation of geothermal heat and power. Our independent analysis and expertise range from geological and reservoir studies, feasibility studies, market assessments, economic forecasting, and geothermal reserves & resources.

GLJ works to accelerate corporate growth and progress geothermal development. We support organizations to improve business strategies, stakeholder engagement and the ability to attract and sustain investors. As the energy sector transforms, GLJ brings peace of mind to clients to enhance their decision making, stakeholder engagements and ensuring success as they move forward.

Acknowledgments

GLJ Ltd. would like to acknowledge Canada's Oil Sands Innovation Alliance (COSIA) and the members of Geothermal working group on their efforts to understand the geothermal potential in the oil sands region of Alberta. Along with the amazing staff at COSIA for facilitating this project, GLJ would like to thank the Geothermal Working group lead, Owen Henshaw (Cenovus Energy) for the advancement and culmination of this study.

GLJ Ltd. would like to thank our partners and the co-authors of this report:

Mehrdad Soltanzadeh, Ph.D., P.Eng.
PetroGem Inc.
Geomechanics

Eric Diggins, P.Eng.
Matthais Kirchhoff, C.Eng., PE
Frontier Project Solutions Ltd.
Drilling and Completions Specialists

George Brindle, P.Eng.
Chantel Moran, P.Eng.
Skoki Project Advisors Inc.
Facilities Design

GLJ Ltd. would also like to thank Tony Pink from NOV for sharing his knowledge on advancing drilling technologies through hard granitic rocks.

I. Introduction

Geothermal resources are abundant and reliable and yet are largely an untapped source of energy. Geothermal extraction technologies are aimed to access natural underground heat from subsurface rocks including sedimentary, volcanic, and hot dry rocks. The extracted energy comes in vapour or liquid to generate electricity using the power generation plants. The amount of available subsurface heat may substantially vary from one region to another depending upon the burial depth, rock types, and proximity to a heat source. As heat varies from region to region, it is important to understand the geology of the field to evaluate geothermal resources.

Over the last decade there has been increased interest in geothermal energy as a source of clean, renewable energy. At the end of 2020, there were 368 geothermal power facilities located around the globe which could provide up to 15,414 MW of electricity capacity (Think GeoEnergy, 2020). Worldwide, these power plants are predominantly in areas with active tectonics and volcanism, such as the “Ring of Fire''. These areas have higher volcanic activity which results in higher heat flow and in turn higher geothermal reservoir temperatures. However, in the last few years, there has been increased interest in the potential for geothermal energy from lower temperature sedimentary basins, as well as pilot projects attempting to unlock the potential from deep hot rocks which have the potential for water to reach a supercritical state.

New extraction technologies have arisen in the last decade which provide opportunities to extract geothermal heat for direct use or electricity generation. Like the oil and gas industry, a technological step change has occurred which has advanced extraction technologies from a conventional sense into an unconventional sense. Three main unconventional technologies exist: Advanced Geothermal Systems (AGS), Enhanced Geothermal Systems (EGS) and Superhot Rock System (SHR) or also referred to as Supercritical Geothermal.

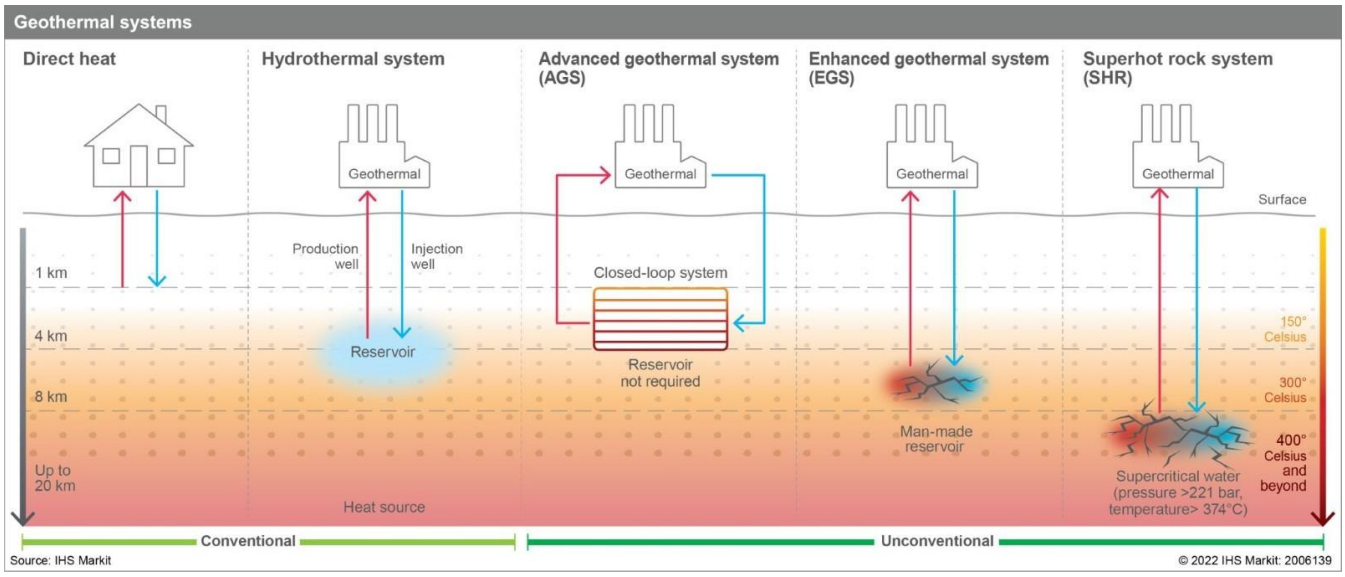

Figure 1: Types of Geothermal systems (IHS Markit, 2022)

AGS extracts heat from the subsurface via conduction without the need of producing water from the formation below. EGS are like conventional geothermal systems with the production of hot water/steam from the subsurface. Unlike conventional geothermal, EGS stimulate the reservoir to create a permeable network to allow fluids to flow from injector and producer wells. The third unconventional technology, SHR or also referred to as

Super Deep Geothermal, is very similar to EGS, however being ~15 kilometers deep with extreme temperatures and pressures, water in the subsurface is potentially in a supercritical phase. Super critical water has an energy carrying capacity of five to ten times the amount of water. In SHR, the energy density is far greater than conventional geothermal systems, AGS and EGS.

Estimates from the geothermal industry have been in the magnitude of 25-45MW of electricity potential from a single well (CATF, 2021). Projects around the world have been attempting to access these SHR resources at shallower depths such as AltaRock in Oregon and the Krafla borehole in Iceland's Deep Drilling Project. However technological challenges exist with drilling at this depth and pressure. Drilling technologies are evolving to allow for deep drilling into crystalline rock such as GA Drilling's PlasmaBit drilling technology, Quaise millimeter wave (MMW) drilling technologies as well as advancements with using conventional drilling techniques in crystalline rock from the FORGE Utah project. These new drilling technologies and trials ultimately aim to reach depths of 10-20 kilometers at a faster rate.

Project Description

Canada's Oil Sands Innovation Alliance (COSIA) and the Geothermal Working Group (WG) is investigating opportunities to generate low carbon heat and power with geothermal in the Oil Sands regions, as geothermal has the potential to generate both low and high-grade heat. Previously, COSIA has commissioned studies that have evaluated at the potential of EGS at ~6km deep as well as AGS with the Eavor technology at ~7km deep. To this point SHR/Super Deep EGS (~15km) has not been considered due to technological challenges with drilling. As new drilling technologies are being explored worldwide and advancements are currently being made, super deep geothermal may be accessible within the next decade.

GLJ and partners are supporting COSIA members to understand the full potential for geothermal resources in the oil sands areas across Alberta by providing a report on the missing unconventional geothermal technology, SHR/Super Deep Geothermal systems.

This report is intended to provide help to COSIA members to make an educated decision on whether to pursue geothermal resources as part of their ESG and innovation strategies. The report is intended to outline the theoretical energy potential obtainable through a super deep geothermal to inform a 2024/2025 deep geothermal drilling project via a Joint Industry Project. This desktop study and report focuses on three main topics: 1) subsurface characterization 2) energy potential calculations, and 3) technoeconomic assessment and technology review.

II. Subsurface Review

Around the world, several superhot rock (SHR) resources are identified as major resources of geothermal energy. (Figure 2: Global superhot drilling and research sites (Sources: Garrison et al., 2020; Hill, 2021).. Examples of these resources are the Geysers, Salton Sea, Pono, and Coso geothermal fields in USA, Kakkonda geothermal field in Japan, Landrello geothermal field in Italy, Krafla, Reykjanes and Hengill geothermal areas in Iceland, Menengai Crater in in Kenya, Los Humeros in Mexico (Petty et al., 2020). These resources are expected to return much more thermal energy compared to the conventional geothermal reservoirs. Nevertheless, the subsurface operations required for exploiting them are more challenging and expensive. Currently, several research and development projects around the world are investigating the potentials, challenges and best practices required for exploiting SHR resources.

Some of these projects are the Japan Beyond-Brittle Project (JBBP) in Japan, the Iceland Deep Drilling Project (IDDP) in Iceland, the Hotter and Deeper Exploration Systems (HADES) in New Zealand, the Integrated Methods for Advanced Geothermal Exploration (IMAGE), Deep Enhanced Geothermal Systems (DEEPEGS) and GEOWELL consortiums in Europe, the Deployment of Deep Enhanced Geothermal Systems for Sustainable Energy Business (DESCRAMBLE) project in Italy, GEMEX in Mexico, and NEWGEN in the USA. This report intends to provide a high-level review of existing knowledge about the mechanical response of SHR, challenges of drilling and hydraulic fracturing operations in these resources, and the potential risk of seismicity induced by stimulating and exploiting them.

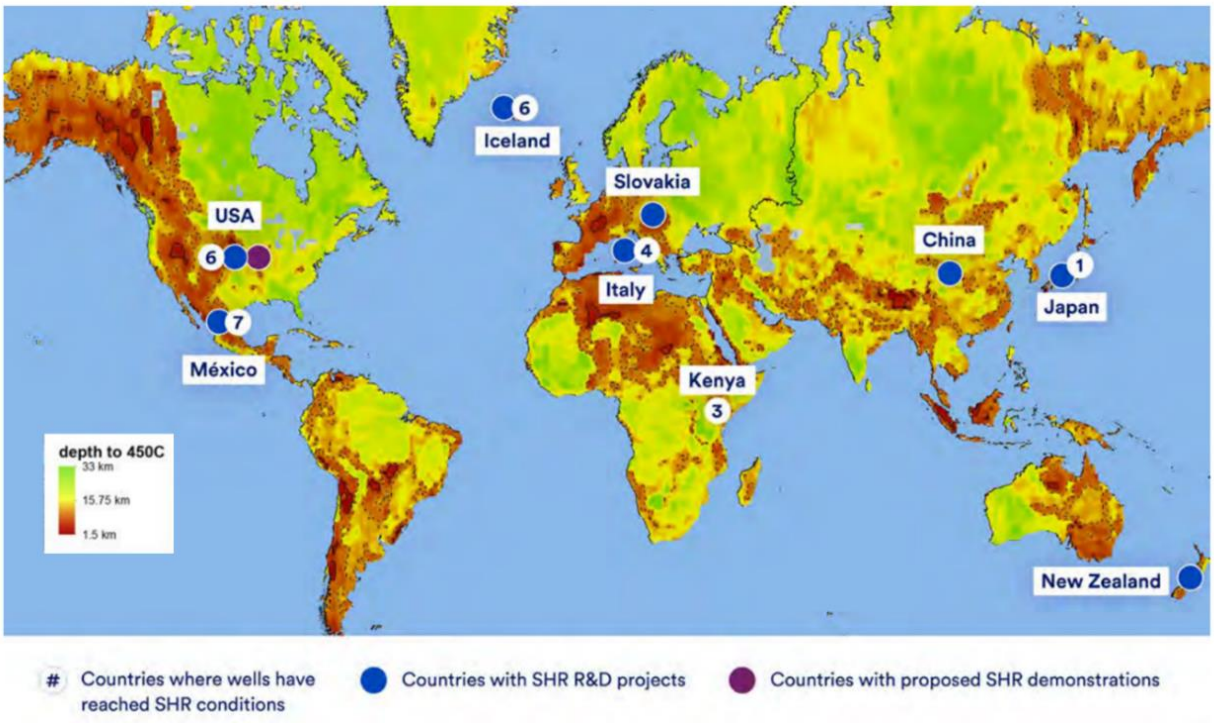

Figure 2: Global superhot drilling and research sites (Sources: Garrison et al., 2020; Hill, 2021).

Geoscience Overview

Within the oil sands region of Alberta, very little to no data exists with regards to the subsurface at great depths. Within the oil sands region, sedimentary rocks currently sit on the Slave Craton. At depths of greater than a few kilometers, it is unknown the composition of rocks in the area, however it is assumed due to current temperature and pressure, rocks would consist of gneisses and schists. The German Continental Deep Drilling program in the 1980s drilled a 10 kilometer deep well through basement rock which encountered mostly paragneiss and metabasites (Emmermann and Lauterjung, 1997).

To reach super critical conditions reservoir temperatures are required to be above 374°C with pressures above 22.1MPa. GLJ assumed a geothermal gradient from a geophysical data from a curie point depth (Gaudreau et al, 2019) as to the temperature (570°C) where magnetic materials undergo a change in their magnetic properties. In the oil sands region, the curie point depth is estimated to be around 25 kilometres ±3 kilometres. This results in

a geothermal gradient of 20-26°C/kilometre. Wells will have to be drilled a minimum of 15 kilometers to reach super critical conditions. Further modelling in this report assumes a 15kilometer minimum depth for a supercritical resource.

Rock Mechanics Superhot Rocks

Supercritical Fluids in Superhot Rocks

The remarkable value of superhot rocks as geothermal resources is related to their supercritical fluid content to an extent that the term 'supercritical geothermal' is widely used by the industry to refer to these rocks. Supercritical water forms when the temperature and pressure is beyond the critical point. This critical point is 374° and 22.1 MPa for pure water but it increases considerably for saline Figure 3. At supercritical conditions, the water is a single-phase fluid that is neither liquid nor gas. Supercritical fluids have high specific enthalpy which makes them very attractive as geothermal resources. For instance, the exploratory well IDDP-1 drilled by the Iceland Deep Drilling Project (IDDP) tapped a reservoir with supercritical water at a temperature of 450 °C and enthalpy of 3.2 MJKg-1 capable of generating 35 MW electrical power from a single well that is multiple times of the 3-5 MW power per conventional wells (Scott et al., 2015). Of course, presence of enthalpy is not enough condition for a supercritical rock system to make it an exploitable SHR geothermal resource. In fact, without a minimum permeability, these resources cannot be economically exploited. A major factor influencing the permeability of SHR is its mechanical behaviour that is reviewed in the following sections.

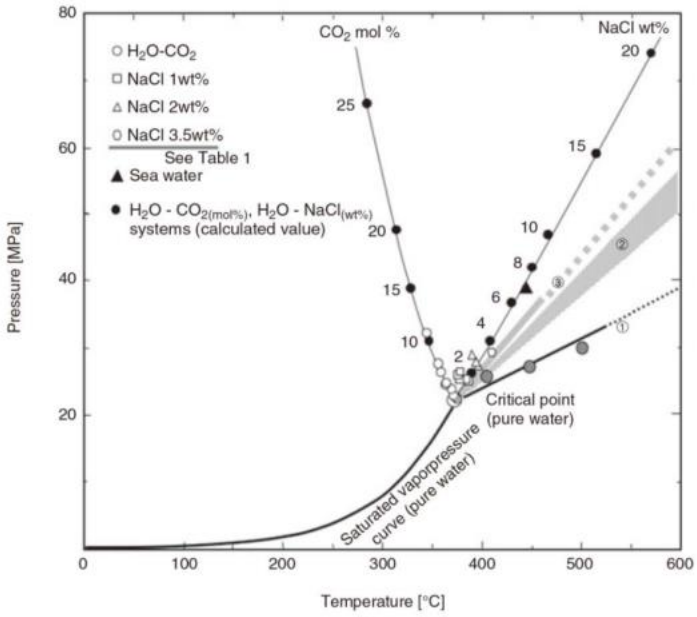

Figure 3: Supercritical state on temperature and pressure diagram for water. Critical points for pure water, saline with NaCl and water with dissolved CO2 are shown on the graph. (Source: Tsuchiya, 2017).

Influence of High Temperatures on Rock Mechanics

Conventional geothermal reservoirs are assumed to be brittle meaning they can only sustain limited deformation before their abrupt failure. Brittle rocks can contain open fractures and they may also be fractured by stimulation. Combination of natural and induced fractures creates pathways that facilitate the convection of the hydrothermal fluid. High temperatures are known to influence rock brittleness. In SHR resources, temperatures can be enough to evolve the mechanical behaviour of the rock from brittle to ductile. Ductile rocks can sustain large deformations without sudden failure. Fractures in these rocks tend to close due to plastic flow in the rock matrix. Therefore,

ductile rocks are expected to include less permeable and open fractures. Therefore, these rocks have less permeability compared to the brittle rocks with open fracture networks.

Graphs in Figure 4 show the results of testing granite samples at high temperatures varying from 600 °C to 1000 °C. These tests are parts of experimenting the mechanical response of rocks in the Japan Beyond Brittle Project (JBBP). The transition from brittle to ductile behaviour of the rock can be clearly observed in these graphs. Brittle response of the samples with lower temperature is captured by an abrupt drop in differential stress. This drop is caused by shear failure and fracturing of the sample. On the other hand, at higher temperatures, the ductile samples keep deforming with less change in differential stress.

The temperatures required for forming brittle-ductile transition varies for different lithologies, ranging from about 360 °C for silicic rocks to 800 °C for non-glassy basaltic rocks (Scott et al., 2015).

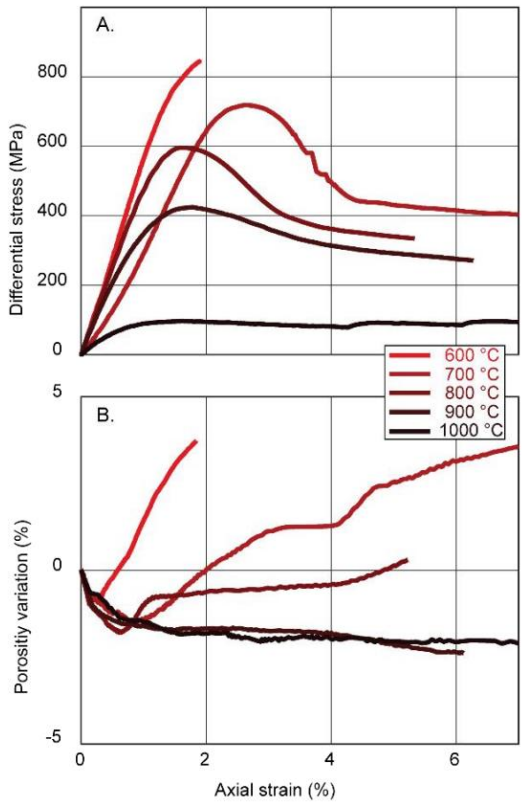

Figure 4: Experimental results of brittle to ductile deformation for granite. The graphs show results of triaxial tests including change of rock porosity and differential stress with increase in axial strain (Source: Acosta et al., 2021).

Brittle-Ductile Transition Zone

The depths at which rock behaviour changes from brittle to ductile is called Brittle-Ductile Transition (BDT) zone. The transition zone is a function of geothermal gradient. This transition does not happen at a certain point but at a range of depths for different reasons such as lithological variation, strain-dependent behaviour of the rock, and in-situ stress magnitude. While at low geothermal gradients the depth of this zone can be more than 10 km, it can be as low as 3 km when the geothermal gradient is high (Tsuchiya, 2017).

As an example, Figure 5 shows the change of brittle to ductile behaviour along the WD-1a well at the Kakkonda geothermal field in Japan. The very high temperature gradient (which is common in Japan), and the lower BDT temperature required for the granite rock result in occurrence of BDT at very shallow depths in this field. This figure shows that transition from brittle rock to a fully ductile/plastic rock occurs through a layer of over one kilometer. Such transition in mechanical behaviour results in major changes in the rock characteristics such as rock deformation and failure, presence and aperture of natural fractures, rock permeability, fracability, stress anisotropy and seismicity as will be discussed in this report.

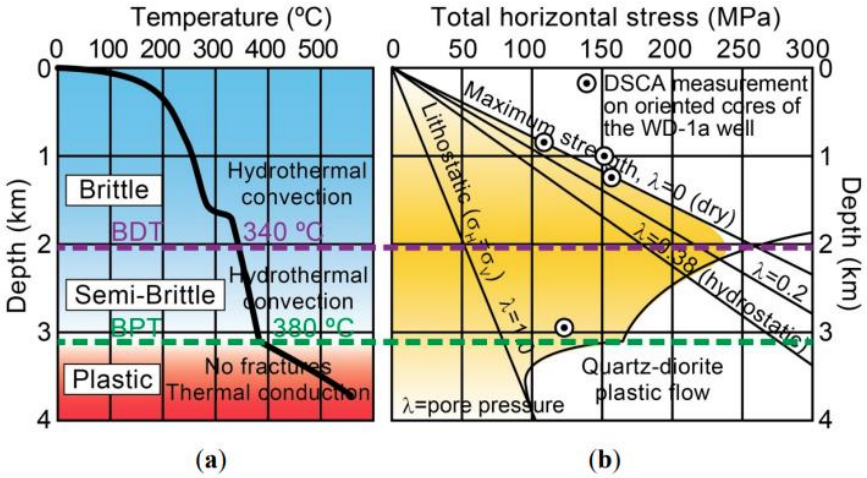

Figure 5: Variations of (a) temperature and (b) total horizontal stress by depth along the WD-1a well at the Kakkonda geothermal field, Japan. BDT is identified on the right graph. λ in the right figure shows pore pressure. (Source: Suzuki et al., 2014)

Variation of Permeability in the Crust

It is known that the rock permeability commonly decreases by depth as the result of changes in porosity and fracture aperture under higher in-situ stresses and the influence of mineral precipitation and hydrothermal alteration. Ingebrigtsen and Manning (1999 and 2010) provided some trends for variation of crustal permeability that are shown in Figure 6a. The trends given in this figure assume the presence of convective hydrothermal flow in brittle crust. However, these authors believe that below BDT the rock permeability cannot be lower than a minimum value between 10-16 to 10-18 m2 (Figure 6b). This value is the minimum permeability required for convective heat transport. On the other hand, Scott at al. (2015) believe a permeability of more than 10-16 m2 is required for potentially exploitable geothermal resources. Comparing the expected permeability of rocks below BDT and the minimum permeability required for geothermal exploitation shows that a critical step in feasibility assessment of superhot geothermal projects is investigating if the influence of BDT on the permeability.

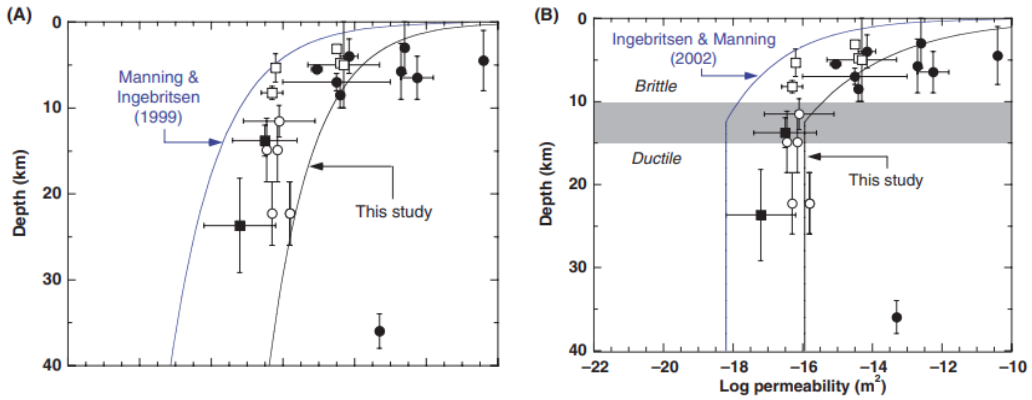

Figure 6: Crustal permeability variation by depth assuming (a) brittle behaviour and (b) brittle-ductile behaviour. The two best fits on the graph represent the estimated trends in 1999 and 2010 (Ingebrigtsen and Manning, 2010)

Permeability in BDT and Its influence on Critical Fluid System

Based on the concepts of supercritical fluids, brittle-ductile transition, and permeability variations, in the feasibility assessment of any superhot geothermal project, the following primary questions need to be answered:

- Does a supercritical fluid system exist?
- Does the target rock have a minimum economical permeability (e.g., 10-16 m2)? Or is it possible to gain such a permeability through stimulation?
- Is the supercritical fluid system influenced by the permeability change in BDT?

As mentioned, low permeability (<10-16 m2) rocks are not expected to result in practically exploitable geothermal systems. On the other hand, modeling by Scott et al. (2015) showed that rocks with high permeability (>10-14 m2) are expected to result in limited supercritical resource development in SHR (Figure 7b, d, and f). In this case, the rate of convective water circulation is high, and water does not reside in the transition zone long enough to reach the supercritical temperatures. The authors conclude that the intermediate permeability values between these two limits (i.e., 10-14 m2 and 10-16 m2) are expected to result in more extensive supercritical resources that are exploitable (Figure 7e and g).

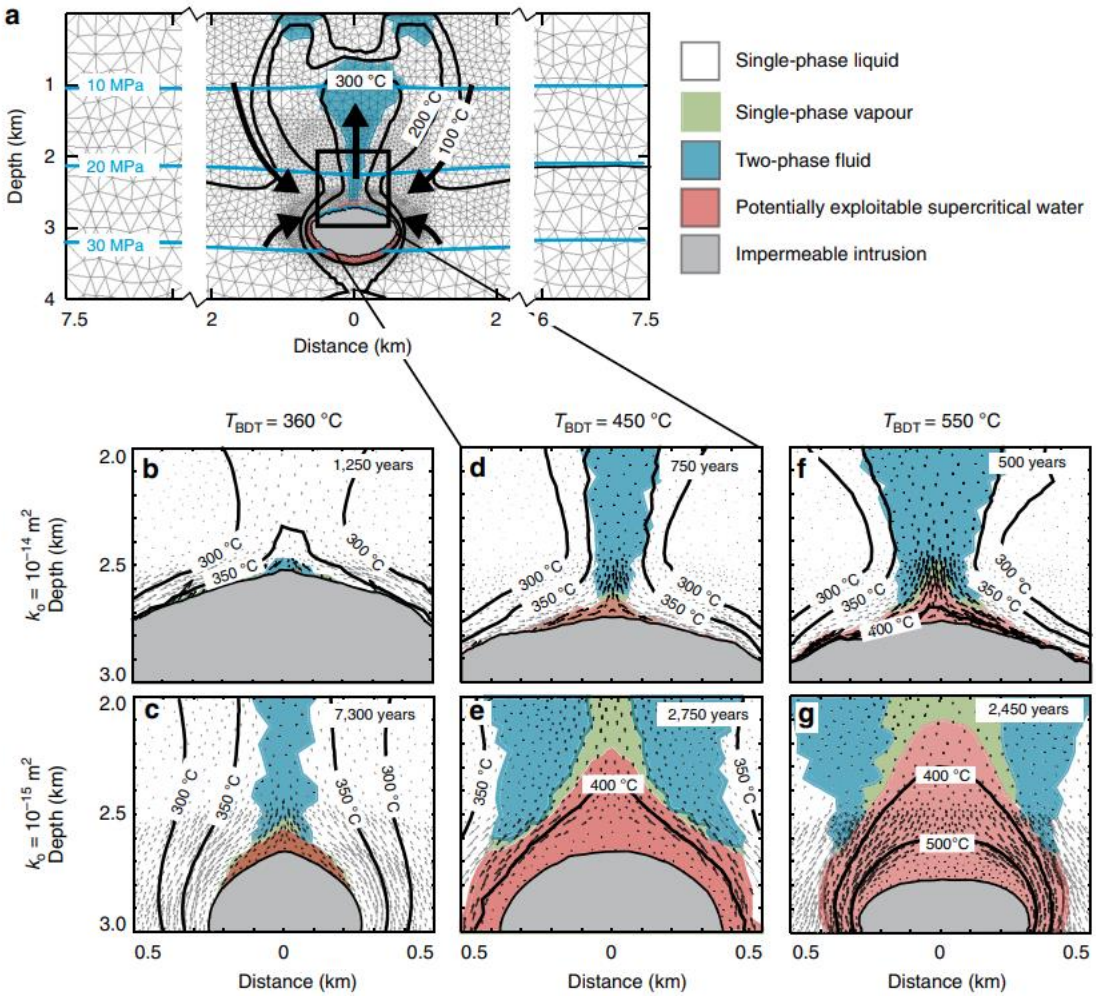

Figure 7: Formation of supercritical water resources depends on geological controls. Potentially exploitable supercritical water regions are identified by red. TBDT is the rock's BDT temperature and k0 is rock permeability (Source: Scott et al., 2015).

With dramatic reduction of rock permeability in BDT, it is critical to examine the possible overlap of this zone with the zone of occurrence of supercritical fluid. If the assumption of very low permeability at the BDT is valid, low BDT temperatures (T_{BDT}<450 °C) can result in formation of minor supercritical resources due to low permeability (Figure 7c) and, therefore, higher T_{BDT} values are required to form exploitable SHR resources (Figure 7e and g).

These conclusions are summarized in Figure 8 that identifies the potentially exploitable supercritical resources based on fluid pressure and temperature, depth of the resource to the top of the magmatic intrusion, and T_{BDT}. From this figure such resources are expected to form in rocks with higher T_{BDT} such as basalt. The graph in this figure also provides the specific enthalpy for these resources. The yellow star on this graph shows the temperature and enthalpy for the IDDP-1 well in Iceland mentioned before.

There are ongoing conversations in the industry about the possibility of having higher than expected permeabilities (i.e., 10^{-16} m^2 or 10^{-18} m^2) in BDT and below it.

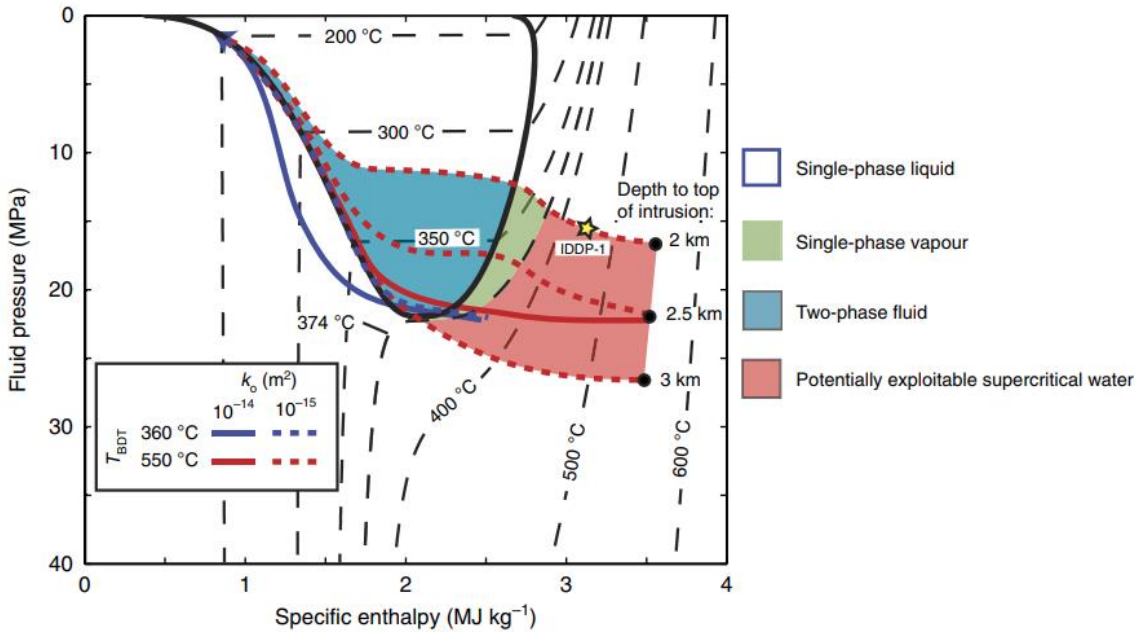

Figure 8: The thermal structure of high-enthalpy systems. The area of exploitable supercritical water is identified by red. The yellow star shows the temperature and specific enthalpy for the IDDP-1 well in Iceland (Source: Scott et al., 2015).

Possible Brittle Behaviour of BDT

Despite the common belief in limited open natural fractures and no potential for fracability of the rocks at BDT, there have been some arguments on the possibility of some brittle behaviour for these rocks. One of the arguments is based on the strain-dependent behaviour of the rock which means rocks show more brittle behaviour at higher strain rates. Scholz (2019) believes that even at the BDT and below it, rock may have a brittle behaviour when the strain rate is very high. Such a high rate may be related abrupt movement of a fault or hydraulic fracturing.

Another factor that is mentioned by Watanabe et al. (2017) states that the common rock behaviour is expected to be different during compaction and expansion (Engvik et al., 2005). This means while the rock response maybe ductile under compressive stresses, it may still show a brittle response to applying tensile forces. Therefore, while creating shear fractures may seem less likely in ductile rock, there may still be a potential for creation of tensile fractures by stimulation.

Another argument is based on the existence of high-permeability (~10^{-15} m^2) ductile crust as observed in some earthquakes, e.g., the 2011 Tohoku-Oki earthquake in northeastern Japan (Okada et al., 2015). There is no evidence that this permeability is permanent and may only be transient at the time of earthquake.

Higher permeability of BDT, or potential for artificial improvement of its permeability through stimulation, can expand the number of potentially exploitable SHR resources especially for the rocks such as granite which have low BDT temperatures at which supercritical fluid condition occurs; in other words, BDT and supercritical system overlap. The graph in Figure 9 shows potentially exploitable SHR geothermal resources (yellow triangle) as function of temperature, depth/effective confining stress, and permeability. This graph identifies the regions of brittle, BDT, and ductile rock behaviour. Five wells drilled in the supercritical fluid systems are also shown on this triangle. Clearly, enhancement of permeability in the BDT and below it can expand the number of potential resources.

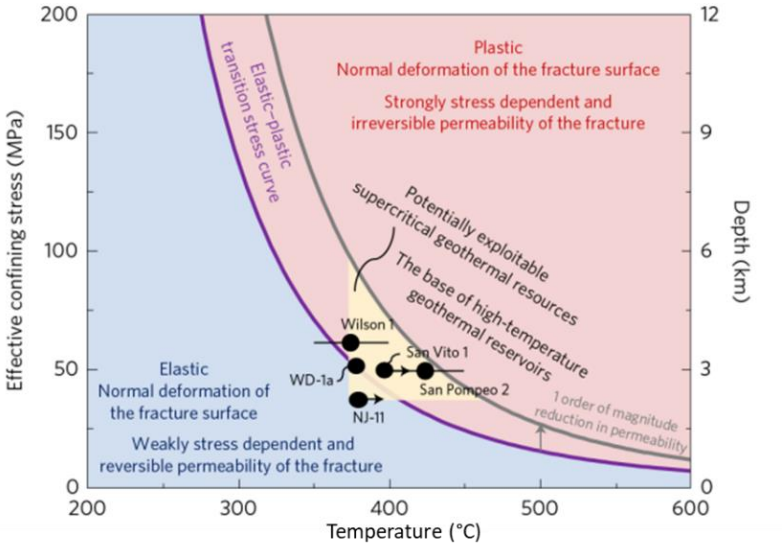

Figure 9: Potentially exploitable supercritical geothermal resources (yellow triangle) as function of rock temperature, depth/confining pressure, and rock BDT (Source: Watanabe et al., 2017).

Possibility of Hydraulic Fracturing in SHR

Stimulation by hydraulic fracturing is very common for conventional hydrothermal reservoirs but its application for superhot rocks is believed to be related to BDT. Rocks with higher T_{BDT} (such as basalt) are usually expected to remain brittle and frackable at the temperature and pressure required for supercritical fluid conditions. On the other hand, rocks with lower T_{BDT} (such as granite) are expected to show ductile behaviour at these conditions meaning less potential for hydraulic fracturing. In the previous section, we reviewed the arguments that claim some degrees of brittleness (and fracability) may exist for these rocks. The mentioned arguments are from the research of Japan Beyond Brittle Project (JBBP) which intends to characterize the brittle-ductile behaviour of granite as the major SHR type in this country. This project has performed several experimental studies to examine the response of granite to hydraulic fracturing at supercritical conditions. Results of some of these laboratory tests are reviewed in the following.

Watanabe et al. (2017) conducted several hydraulic fracturing experiments at 200-450 °C by injecting water into cylindrical granite samples at the common triaxial test stress state. Tests showed intensive fracturing at all temperatures, but the fracturing characteristics changed with temperature. While fewer planar fractures were created at the lower temperatures, a substantial number of shorter fractures were formed inside the entire sample (Figure 10). These densely distributed short fractures are called cloud-fracture networks (Watanabe et al., 2018). These fractures are believed to be the microfractures in the granite sample which existed before testing and were re-opened by stimulation. This mechanical response was accompanied with drastic changes in the breakdown pressure as temperature varied. For example, breakdown pressure changed from the twice of confining pressure for the lowest temperature to much lower pressures (close to confining pressure) for the highest temperature as shown in Figure 11. The authors believe this significant change in behaviour is related to the reduction in the viscosity of the injected water. However, ductile behaviour of the granite and possible stress redistribution (discussed later in this report) may be other factors leading to these results.

These experiments also showed rock permeability improvement at all temperatures including the temperatures exceeding the critical temperature of water. The improved permeability at the supercritical and BDT temperatures was about 2x10-15 m2 which is expected to result in a productive SHR reservoir according to the minimum

requirement of 10-16 m2 suggested by Scott et al. (2015). The conclusion of these experiments was that rocks can be hydraulically fractured to improve the permeability even at temperatures greater than TTBD. The stimulated fractures in these rocks, however, are not the usually expected planar hydraulic fractures or critically stressed shear fractures but they are cloud-fracture.

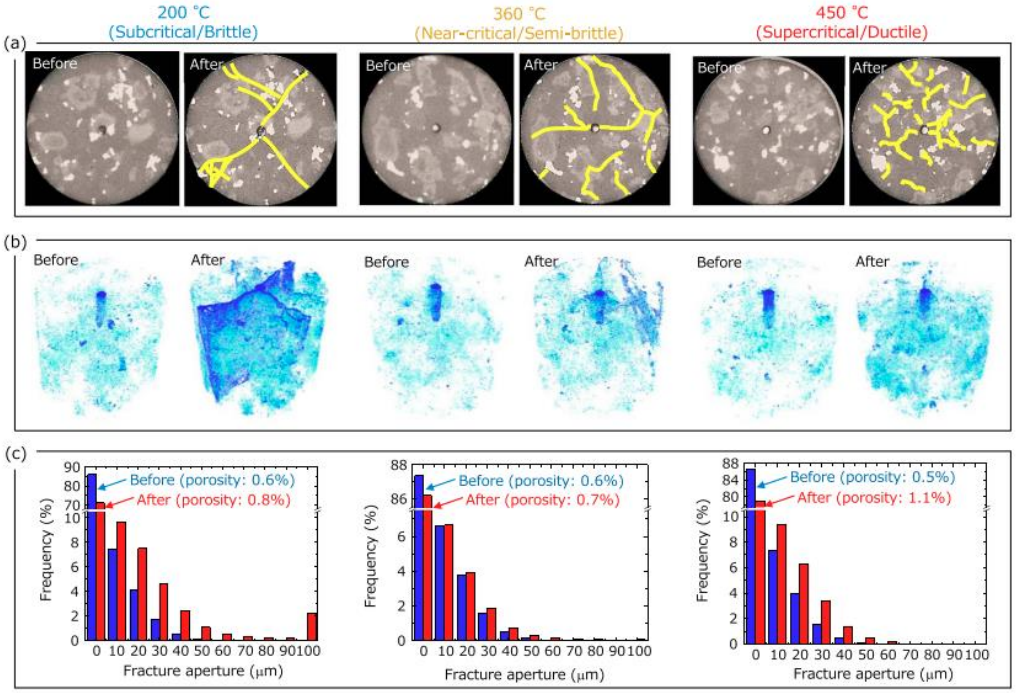

Figure 10: Results of hydraulic fracturing experiments on the granite samples showing (a) CT images, (b) fracture aperture distribution from the CT data, and (c) histograms of the fracture aperture with porosity values for the samples before and after experiment at 200, 360, and 450 °C (Source: Watanabe et al., 2017).

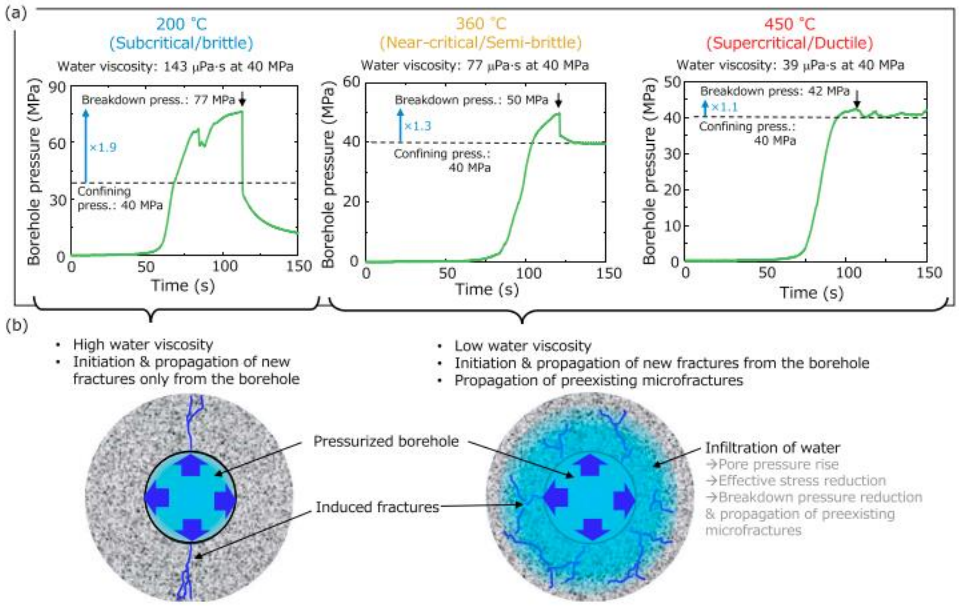

Figure 11: Results of hydraulic fracturing experiments on granite samples showing (a) pressure curves and breakdown pressure during the experiment, and (b) two types of fracturing mechanisms (Source: Watanabe et al., 2017).

In a later study, Watanabe et al. (2018) performed high-temperature hydraulic fracturing experiments in a true triaxial stress state for cubic granite samples. In true triaxial tests the stresses acting on the sample can be different in three different orientations (anisotropic) as it is common in the earth crust. The results of these tests also showed the formation of cloud-fracture network at relatively low injection pressure between the intermediate and minimum principal stresses in a normal stress regime (Figure 12). This study also concluded the possibility of well stimulation for effective production from SHR reservoirs. Further tests were conducted on the granite samples confirming similar results (e.g., Goto et al., 2021).

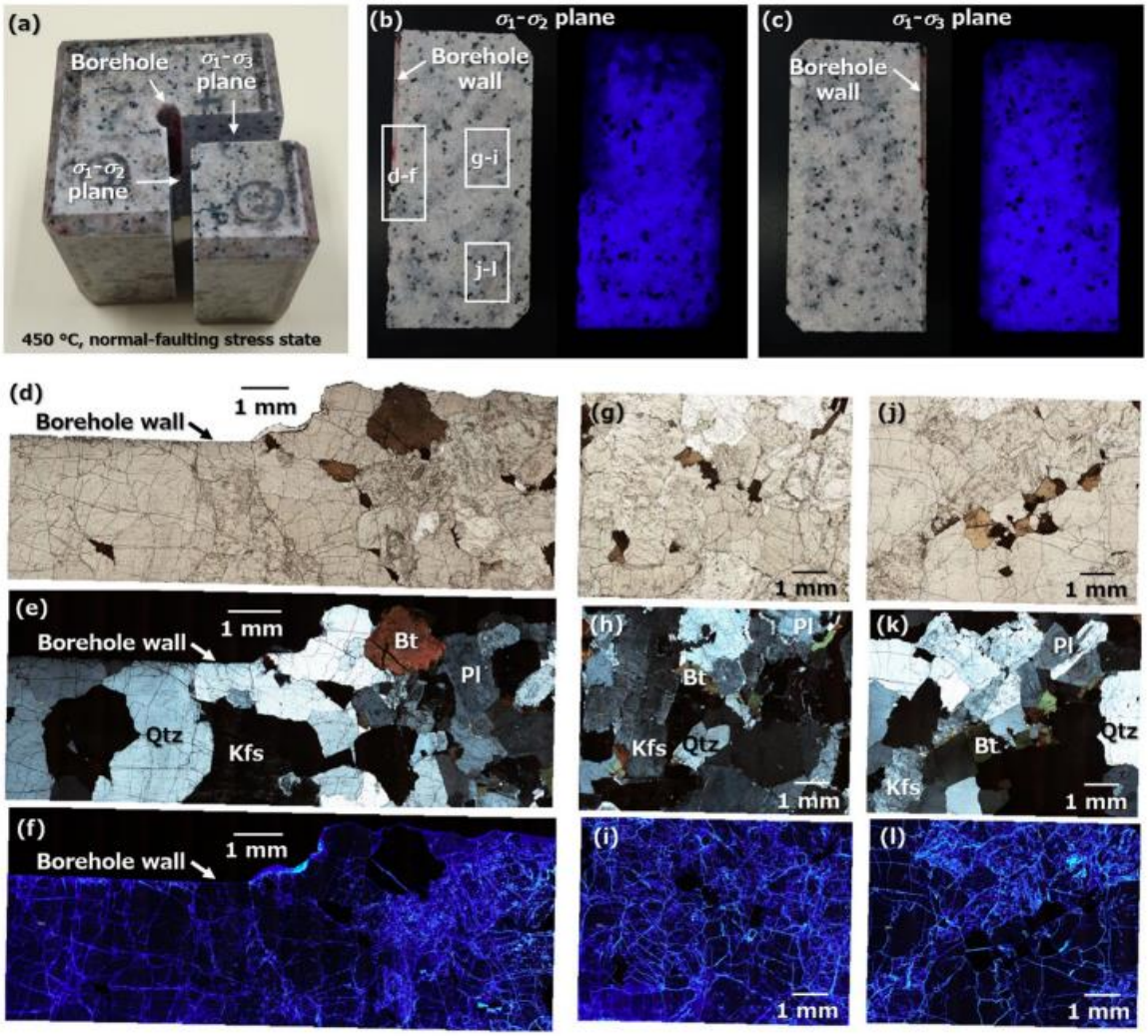

Figure 12: Cloud-fracture networks formed during experimental hydraulic fracturing experiments on cubic samples. The samples tested in true triaxial apparatus under normal-faulting stress regime and at 450 °C (Source: Watanabe et al., 2018).

In-situ Stresses in BDT

In-situ stresses are among the most important geomechanical parameters. For instance, the stability of drilling, and orientation, geometry, and conductivity of hydraulic fractures are all closely related to these stresses. Also, natural fractures and their aperture/conductivity, as important contributors to performance of a reservoir, are related to the stress state in the rock. In-situ stresses in the rocks are related to different factors such as overburden pressure, tectonic forces, fluid pressure, and temperature, and of course, rock mechanical behaviour. In-situ stress tensor in the earth is commonly defined using three stress components, i.e., vertical stress or

overburden pressure, and two horizontal stresses. In brittle/elastic rocks, the magnitudes of these three components can be different (i.e., anisotropic) and functions of rock deformability and faulting regime. In ductile rocks, however, plastic flow has a significant influence on the stress components and can result in more isotropic stresses where the stress component magnitudes are closer to each other. Therefore, superhot rocks in BDT and below it is expected to show more isotropic stresses.

Figure 5: Variations of (a) temperature and (b) total horizontal stress by depth along the WD-1a well at the Kakkonda geothermal field, Japan. BDT is identified on the right graph. λ in the right figure shows pore pressure. (Source: Suzuki et al., 2014)b shows a sketch of variation of horizontal stress by depth in BDT and below it in Kakkonda geothermal field, Japan. While this component is much greater than the overburden pressure (or vertical stress) in the brittle zone, it drastically decreases in BDT until, eventually, in the ductile zone these stress components become close (i.e., isotropic) as the result of plastic flow. As mentioned, less anisotropic stress state can influence natural fracture networks, drilling, and hydraulic fracturing. It also can influence potential for seismicity in a field. Therefore, proper characterization of in-situ stresses in BDT is critically important for SHR.

Induced Seismicity in SHR

Induced seismicity has been observed in many geothermal fields around the world. Table 1 includes multiple cases of induced seismicity around the world which were caused by stimulating and exploiting geothermal resources. One prominent example is a 2018 earthquake with the magnitude of 5.4 in Pohang, South Korea that caused extensive structural damage and even injuries (Kim et al., 2018). This event which is one the largest known induced earthquakes in the world caused by stimulation of the EGS. Other major examples of large earthquakes related to exploiting geothermal reservoirs are magnitude of 5.0 at the Geysers geothermal field (Majer et al., 2017), magnitude of 4.0 in the Hellisheidi geothermal field, Iceland (Juncu et al., 2018), and magnitude of 3.4 in Basel, Switzerland (Häring et al., 2008).

In contrary to conventional geothermal and hydrothermal operations, SHR geothermal resources are usually expected to experience less induced seismicity if they are formed in BDT or below it. This means faults located in ductile rocks are expected to show less seismogenic behaviour since less seismic energy nucleation and accumulation is expected to occur in these rocks. This behaviour can be explained by seismogenic windows (Scholz, 2019) which, for every rock, defines a range of temperature at which the rock is brittle enough to create a seismic response. For instance, this window for the granite rock is between 90 °C to 350°C. In fact, some SHR with very high temperature seem to agree with this theory as they show low seismic activity at high temperatures close to TBDT. Examples of these SHR resources are:

- Geysers geothermal field, California (400 °C): For this field, seismic activity stops at 4 km depth. This depth corresponds to the start of the temperature corresponding to BDT (Ground Water Protection Council and Interstate Oil and Gas Compact Commission, 2012).
- Krafla Geothermal Area, Iceland (345 °C): Most of the seismicity in this area is located above 2.7 km depth and only very few are below 3 km (Ágústsson et al., 2012). This depth is close to the BDT for this area which is as shallow as 2.7 km depth (Flóvenz et al., 2015).
- Coso Geothermal Field, California (300 °C): In this field, the abrupt decrease of seismicity at certain is speculated to be relate to BDT.

These cases, however, do not rule out mean the chance of induced seismicity at and below BDT. For instance, Salton Sea Geothermal Field, California (390 °C) with BDT as shallow as 2 km depth showed frequent seismicity below this depth (Lohman and McGuire, 2007). In addition, Acosta et al. (2021) challenge the improbability of induced seismicity by experimental tests which showed earthquakes may be created at temperatures higher than

the upper limit of the seismogenic window suggested by Scholz (2019). For instance, their results show that laboratory faults can become unstable at temperature of 500 °C in granite which is higher than the upper bound of seismogenic window for this rock. The arguments on brittleness of BDT (as presented in Section 8) may also be used here to also argue for the potential for induced seismicity within and below this zone. In addition, studies show that injection of cold-pressurized fluid into the superhot rock strongly changes the seismogenic behaviour of the reservoir faults and magnitude of induced seismicity (Acosta et al., 2021)

In conclusion, although the potential for induced seismicity is expected to be less for SHR, possibility of induced seismicity cannot be completely ruled out. Therefore, each project needs to be individually evaluated and proper risk management procedures and guidelines will be required.

Table 1: Overview of the induced seismicity cases in geothermal reservoirs. The table includes the following factors: d: depth (km), T: reservoir or aquifer temperature (°C), dT: temperature difference between (re)injected fluid and reservoir temperature, db: depth of the basement (km), Φ: average matrix porosity, M: maximum magnitude (NR = no seismicity reported), dV_net: net injected (positive) or produced (negative) volume, dP: maximum injection pressure (Source: Buijze et al., 2019).

	case	region	type	d	T	dT	rocktypy	db		start	M	dV_net	dP_i	tectonic
1	Habanero 1 2003	Cooper Basin	EGS	4.4	250	220	Granite	3.6	0.01	7-11-2003	3.7	2.0E+04	70	TF
2	Habanero 1 2005	Cooper Basin	EGS	4.4	250	220	Granite	3.6	0.01	10-9-2005	3	2.3E+04	62	TF
3	Habanero 4 2012	Cooper Basin	EGS	4.1	240	210	Granite	3.6	0.01	14-11-2012	3	3.4E+04	50	TF
4	Jolokia	Cooper Basin	EGS	4.8			Granite	3.6	0.01	23-10-2010	1.6	3.8E+02	70	TF
5	Rosemanowes	Cornwall	EGS	2.6	95	65	Granite	2			2			
6	The Geysers	Geysers	GF	3.0	400		Metamorphic	3.3	0.04	1-1-1960	5	-2.0E+09	0.1	NF-SS
7	Coso	Great Basin	GF	3.5	285		Crystalline			1-1-1987	4.4	-5.5E+08		NF-SS
8	Brady Hot Springs	Great Basin	GF-EGS	1.8	193		Metamorphic	1.2	0.01	1-1-1920	2.2			NF-SS
9	Desert Peak EGS 2013	Great Basin	GF-EGS	1.7	207	177	Metamorphic	2	0.04	15-1-2013	1.6	2.0E+04	10.3	NF-SS
10	Desert Peak EGS 2011	Great Basin	GF-EGS	1.1	195		Metamorphic	2	0.09	1-4-2011	0.7	1.3E+05	8	NF-SS
11	Hellisheidi	Iceland Volcanic Zones	GF	2.5	235	165	Basalt	0	0.03	1-9-2011	4		2.8	NF-SS
12	Nesjavellir	Icelandic Volcanic Zones	GF		380		Basalt			1-1-1987	3.2			
13	Svartsengi	Icelandic Volcanic Zones	GF	2.0	260	180	Volcaniclastic	0.4		1-1-1976	3.2			NF
14	Reykjanes	Icelandic Volcanic Zones	GF		345		Volcaniclastic			1-1-2006	3			NF
15	Krafla	Icelandic Volcanic Zones	GF	2.1	440		Basalt	2.1		1-1-1977	2		0.3	NF
16	Laugarnes	Icelandic Volcanic Zones	GF											
17	Yanaizu Nishiyama	Japan	GF	2.6	341		Volcaniclastic			1-5-1995	4.9			
18	Sankt Gallen	Molasse Basin	HSA	4.3	145	115	Carbonate	4.8	0.06	19-7-2013	3.5	1.0E+03	9	SS
19	Unterhaching	Molasse Basin	HSA	3.4	122		Carbonate	3.7	0.05	1-10-2007	2.4	0.0E+00	1	TF-SS
20	Poing	Molasse Basin	HSA	3.1	85		Carbonate	3.2	0.05	1-12-2012	2.1	balanced	1	TF-SS
21	Geinberg	Molasse Basin	HSA	2.1	105		Carbonate	2.9	0.03	1-1-1980	NR	balanced		TF-SS
22	Geinberg	Molasse Basin	HSA	2.2	105		Carbonate	2.9	0.03	22-12-1998	NR		0.2	TF-SS
23	Pullach	Molasse Basin	HSA	3.4	107	45	Carbonate	3.5	0.05	1-1-2006	NR	balanced	1.5	TF-SS
24	Californië CWG	Netherlands	HSA	2.1	82	47	Carbonates & SAndstones	3	0.03	20-1-2013	NR			
25	Honselersdijk	Netherlands	HSA	2.4	89	59	Sandstone	6.5	0.16	8-5-2012	NR	balanced		
26	Koekoekspolder	Netherlands	HSA	1.9	76	45	Sandstone	4.5	0.18	10-9-2011	NR	balanced		
27	Gross Schoenebeck water-frac	North German Basin	HSA-HF	4.1	150	120	Volcaniclastic	4	0.09	9-8-2007	-1	1.3E+04	58.6	NF-SS
28	Gross Schoenebeck 4120 gel	North German Basin	HSA-HF	4.1	150	120	Sandstone	4	0.09	18-8-2007	NR	5.0E+02	49.5	NF-SS
29	Gross Schoenebeck 4120 gel	North German Basin	HSA-HF	4.2	150	120	Sandstone	4	0.09	19-8-2007	NR	5.0E+02	38	NF-SS
30	Hannover GeneSys waterfrac	North German Basin	HSA-HF	4.2	169		Sandstone	5	0.07	23-5-2011	NR	2.0E+04	47	NF
31	Horstberg GeneSys	North German Basin	HSA-HF	4.2	158		Sandstone	5	0.07	23-10-2003	NR	2.0E+04	34	
32	Neubrandenburg	North German Basin	HSA	1.2	54		Sandstone	5.5	0.3	1-1-1989	NR			
33	Neuruppin	North German Basin	HSA	2.4	64		Sandstone	5.5	0.25	1-1-1987	NR			
34	Neustadt-Glewe	North German Basin	HSA	2.5	99	49	Sandstone	5.5	0.22	1-1-1994	NR		0.5	
35	Waren	North German Basin	HSA	1.6	61	30	Sandstone	5.5	0.28	1-1-1985	NR			
36	Sonderborg	North German Basin	HSA	1.2	48	36	Sandstone	3	0.28	1-1-2013	NR			
37	Margretheholm	Norwegian Danish Basin	HSA	2.6	73	55	Sandstone	2.6	0.2	1-1-2005	NR		6	
38	Thisted	Norwegian Danish Basin	HSA	1.3	45	33	Sandstone	4.8	0.26	1-1-1984	NR		1.7	
39	Hódmezővásárhely	Pannonian Basin	HSA	2.3	90	55	Sandstone	6	0.15	1-1-1954	NR		0.3	TF-SS
40	Orosháza-Gyopárosfürdő	Pannonian Basin	HSA	1.6	88	45	Sandstone	4	0.21	1-1-2011	NR		0.5	TF-SS
41	Szentes	Pannonian Basin	HSA	2.3	90		Sandstone	5	0.21	1-1-1958	NR	3.0E+08		TF-SS
42	Paris Basin Average	Paris Basin	HSA	1.9	67		Carbonate	2.5	0.15	1-1-1970	NR		1	NF
43	Pohang (PX-1 + PX-2)	Pohang Basin	EGS	4.2	140	110	Granodiorite	2.4	0.01	29-1-2016	5.4	1.3E+04	89.2	TF-SS
44	Uniejow	Polish Lowlands	HSA	2.0	68	35	Sandstone	5.5	0.19	1-1-2001	NR		0.7	
45	Salton Sea	Salton Sea	GF	2.5	390		Sands & Shales	5.5	0.07	1-1-1986	5.1	-4.5E+08		NF-SS
46	Rotokawa	Taupo Volcanic Zone	GF	2.2	340	210	Volcaniclastic	2.5	0.11	1-1-1997	3.3			
47	Kawerau	Taupo Volcanic Zone	GF	2.1	320	200	Metamorphic	2.6	0.15	1-1-1957	3.2			
48	Mokai	Taupo Volcanic Zone	GF	2.4	326	100	Volcaniclastic		0.2	1-1-2000	3.2			
49	Ngatamariki	Taupo Volcanic Zone	GF	3.0	280		Volcaniclastic		0.1	1-1-2013	2.7			SS
50	Wairakei-Tauhara	Taupo Volcanic Zone	GF	2.9	260		Various		0.08	1-1-1958	2.5		5	
51	Ngawha	Taupo Volcanic Zone	GF	1.5	250		Metamorphic		0.05	1-1-1998	NR			
52	Ohaaki	Taupo Volcanic Zone	GF	3.0	265		Volcaniclastic		0.15	1-1-1988	NR			
53	Monte Amiata Piacastl.	Tuscany-Latium	GF	3.5	300		Metamorphic			1-1-1969	4.5			TF
54	Larderello circulation	Tuscany-Latium	GF	2.0	250		Carbonate	3	0.03	1-1-1905	3.2			NF
55	Torre Alfina RA1	Tuscany-Latium	GF	1.7	210		Carbonate			27-1-1977	3	4.9E+03	1.2	NF
56	Latera Well L2 test	Tuscany-Latium	GF	1.5	230		Carbonate			15-3-1980	1.9	3.0E+04	6	
57	Latera L1 test 1981	Tuscany-Latium	GF	1.7	230		Carbonate			22-6-1981	0.5	3.6E+03	7	
58	Latera L1 test 1982	Tuscany-Latium	GF	1.7	210		Carbonate			2-2-1982	0.4	9.2E+03	7	
59	Basel	Upper Rhine Graben	EGS	4.8	190	160	Granite	2.6	0.01	2-12-2006	3.4	1.2E+04	29.6	SS
60	Soultz-sous-Forêts GPK3 2003	Upper Rhine Graben	EGS	5.1	200	170	Granite	1.4	0.02	27-5-2003	2.9	3.7E+04	18	NF-SS
61	Soultz-sous-Forêts GPK4 2005	Upper Rhine Graben	EGS	5.2	200	170	Granite	1.4	0.02	7-2-2005	2.7	1.2E+04	18	NF-SS
62	Landau	Upper Rhine Graben	EGS	3.2			Multiple	2.7	0.01		2.7			
63	Soultz-sous-Forêts GPK2 2000	Upper Rhine Graben	EGS	5.0	200	170	Granite	1.4	0.02	30-6-2000	2.5	2.3E+04	13	NF-SS
64	Insheim stimulation	Upper Rhine Graben	EGS	3.6	160		Multiple	3.5	0.05	7-4-2010	2.4	9.0E+03	9	NF-SS
65	Soultz-sous-Forêts GPK4 2004	Upper Rhine Graben	EGS	5.2	200	170	Granite	1.4	0.02	13-9-2004	2.3	9.3E+03	17	NF-SS
66	Insheim production	Upper Rhine Graben	EGS	3.6	160	115	Multiple	3.5	0.05	13-10-2012	2.1	balanced	1.2	NF-SS
67	Soultz-sous-Forêts GPK1 1993	Upper Rhine Graben	EGS	3.6	160	130	Granite	1.4	0.02	1-9-1993	1.9	4.5E+04	19	NF-SS
68	Rittershoffen GRT-1 hydraulic stimulation	Upper Rhine Graben	EGS	2.6	160		Granite	2.2	0.01	27-6-2013	1.6	4.1E+03	3	NF
69	Rittershoffen circulation	Upper Rhine Graben	EGS	2.6	170		Granite	2.2	0.01	1-9-2016	1.3	0.0E+00	0.8	NF
70	Rittershoffen GRT-1 thermal stimulation	Upper Rhine Graben	EGS	2.6	160	148	Granite	2.2	0.01	23-4-2013	1.2	4.2E+03	2.8	NF
71	Soultz-sous-Forêts GPK2 1995	Upper Rhine Graben	EGS	3.8	165	135	Granite	1.4	0.01	16-6-1995	0.3	2.3E+04	12	NF-SS
72	Bruchsal	Upper Rhine Graben		2.5	134	74	Sandstone	2.85	0.06	1-1-2002	NR	0.0E+00	0.5	NF-SS
73	Vierpolders	West Netherlands Basin	HSA	2.1	85	61	Sandstone	5	0.2	23-9-2015	NR			

III. Energy Potential

Heat-In-Place Modelling

Heat-In-Place Modelling is the basis to understanding geothermal potential. Heat-In-Place is calculated to determine the available thermal energy, which is an analogous to a volume in place calculation for hydrocarbon recovery. GLJ utilized a typical EGS pad design to aid in calculating thermal energy in place. Input parameters such as temperature, thickness and rock type were a generic distribution of values as the rock type is unknown.

Heat-In-Place Modelling - Theory

The volumetric method of using stored Heat-In-Place to assess geothermal potential was first presented by the United States Geological Survey (White and Williams, 1975). The refinement of the methodology, such as including Monte-Carlo simulation has occurred over the years, however, the fundamental approach is still the same and is commonly used for geothermal projects to this day.

The first step to estimate the volumetric Heat-In-Place is to calculate the stored energy in the earth. Understanding the reservoir parameters and properties are vital. The geological parameters needed to calculate stored energy are porosity, temperature, bulk volume, and specific heat capacities of rock. The stored energy in the earth can be defined as thermal energy (Q_r)and is calculated using the following formula:

$$\boldsymbol{Q_r} = \left[(\boldsymbol{V_n} * \boldsymbol{Cp_r}) + \left(\boldsymbol{V_f} * \boldsymbol{Cp_f}\right)\right] * (\boldsymbol{T_r} - \boldsymbol{T_0})$$

Q_r = Thermal Energy (MJ)
V_n = Net Rock Volume (m^3)
V_f = Net Fluid Volume (m^3)
Cp_r = Specific Heat capacity of the Rock (MJ/m^3K)
Cp_f = Specific Heat capacity of the Fluid (MJ/m^3K)
T_r = Reservoir Temperature (K)
T_0 = Reinjection Temperature (K)

A recovery factor is applied to calculate the thermal energy to be potentially extracted from the reservoir. GLJ has estimated recovery factor at 10-25% for sedimentary rocks based on the formula proposed by Lavigne and Maget (1977) which has been corroborated by many authors, such as Williams (2007). Recovery factor can be characterized by the following formula:

$$\boldsymbol{\gamma} = \frac{\boldsymbol{T_r} - \boldsymbol{T_{min}}}{\boldsymbol{3} * (\boldsymbol{T_r} - \boldsymbol{T_0})}$$

γ = Recovery Factor
T_r = Reservoir Temperature (K)
T_{min} = Minimum Facility Temperature (K)
T_0 = Rejection Temperature (K)

Recovery factor can be multiplied by thermal energy to obtain the wellhead thermal energy (Q_{wh}), defined as the energy which is available at surface. Wellhead Thermal Energy is defined by the following formula:

$$\boldsymbol{Q_{wh}} = \boldsymbol{\gamma} * \boldsymbol{Q_r}$$

Q_{wh} = Wellhead Thermal Energy (MJ)
Q_r = Thermal Energy (MJ)
γ = Recovery Factor

Q_{wh} can be divided by the typical geothermal life cycle (e.g., 30 years) to calculate the electrical power production potential of the area.

$$MW_t = Q_{wh}/Time$$

MW_t = Gross Wellhead Thermal Energy (MW_t)
Time = Time (seconds)

Heat-In-Place Modelling - Results

GLJ utilized the Heat-In-Place calculations and applied this to a Monte-Carlo simulation. The input parameters used in the calculations were defined by P90 to P10 distributions. Below in Table 2 are the input parameters used to calculate heat is place. Yellow cells are input values, while white cells are a calculated or a constant value.

The Monte-Carlo Heat-In-Place model was run using 10,000 iterations. Over a 40-year time frame, the mean value for Gross Wellhead Thermal Energy equated to 52.0MW with the high probability (P90) being at least 42.1MW and the low probability (P10) equating to 61.8MW for the Pad area.

Figure 13: Diagrammatic drawing of well placement for high flow rate case design. Wells are 500m apart with a 300m width and a production/injection interval of 1000-1500metres.is a diagrammatic drawing of the injector producer combination, which was used for the volume of the heat in place modelling. Table 2: Heat-In-Place modelling results of high flow rate case. is the heat-in-place modelling inputs and results.

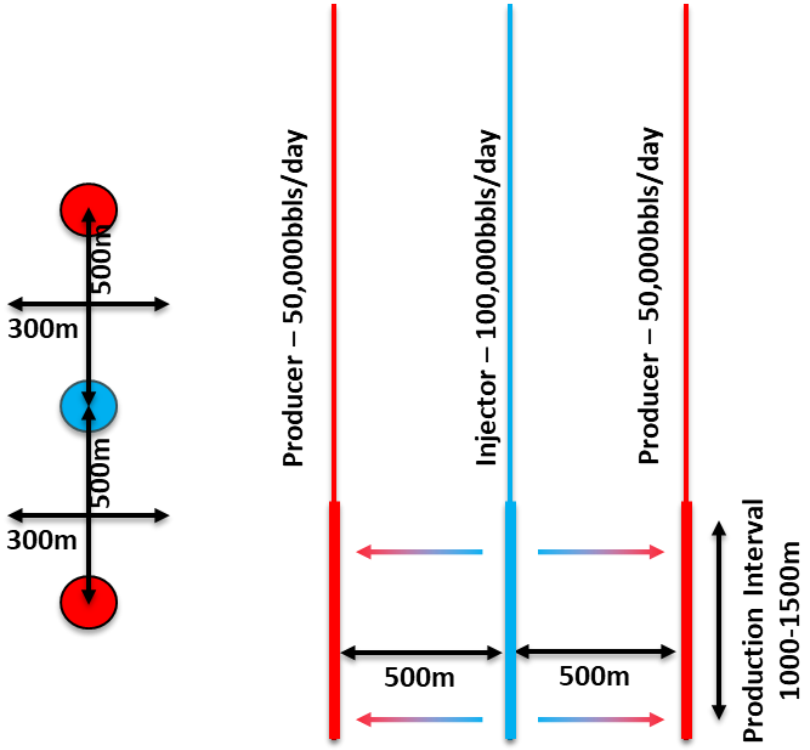

Figure 13: Diagrammatic drawing of well placement for high flow rate case design. Wells are 500m apart with a 300m width and a production/injection interval of 1000-1500metres.

Table 2: Heat-In-Place modelling results of high flow rate case.

Inputs

Variable	Symbol	Unit	Low Est. (P90)	Mean	High Est. (P10)
Distance from Injector to Producer	X	m		**500**	
Width of Injection	Y	m		**300**	
Well Length	L	m	1000	**1250**	1500
Number of Injectors				**1**	
Number of Producers				**2**	
Gross reservoir volume	V_g	m^3	311,338,516	**375,000,000**	438,094,092
Bulk Reservoir Volume	V_b	m^3	308,778,397	**372,032,507**	434,758,413
Porosity	ϕ	v/v	0.005	**0.008**	0.010
Net Rock volume	V_n	m^3	306,044,893	**369,242,263.28**	430,556,495
Fluid Volume	V_f	m^3	1,955,619	**2,790,244**	3,681,407
Rock Volumetric Heat Capacity	Cp_r	MJ/m^3K	2.2	**2.3**	2.4
Reservoir Fluid Heat Capacity	Cp_f	kJ/kgK	2.6	**2.65**	2.7
Reservoir Temperature	T_r	K		**673.15**	
Rejection Temperature	T_0	K		**333.15**	
Minimum Facility Temperature	T_{min}	K	583.15	**588.15**	593.15
Injection Water Density		Kg/m3		**950**	
Reservoir Water Density		Kg/m3		**750**	
Time	Time	Years		**40**	

Outputs

Variable	Symbol	Unit	Low Est. (P90)	Mean	High Est. (P10)
Thermal Energy	Q_r	MJ	243,247,750,019	**291,261,459,554**	339,142,011,646
Wellhead Thermal Energy	Q_{wh}	MJ	53,702,273,923	**65,533,828,400**	77,974,722,323
Gross Wellhead Thermal Energy	MW_{th}	MW	42.6	**52.0**	61.8

Super Hot Rock Geothermal Systems Modelling

Super Hot Rock Pad Design

SHR geothermal assumes an enhanced geothermal system design for the primary extraction method to be investigated in this study. EGS, like conventional geothermal systems, use a combination of injector and producer wells. In this case, the designed EGS system uses a vertical injector and producer combination with one injector and two producers. The number of production and injection wells will be dictated by the facilities needs.

GLJ has assumed injected water disperses into the reservoir equally in both directions, perpendicular to the injector. The initial spacing was selected at 500metres based of historic EGS projects. This distance is also to be investigated in modelling. To increase flow into and out of the formation, wells are assumed to be hydraulicly stimulated to increase permeability.

Thermal Displacement Modelling – Theory

Energy in a Geothermal system is stored in the rock, particularly in systems of low or no natural porosity. Geothermal injection and production are essentially sweeping the thermal energy out of the rock using water. In conventional geothermal systems heat can be transferred from outside of the production/injection wells via natural permeability and convection. However, in an EGS or SHR system, natural permeability is minimal or

nonexistent, so the replenishment of heat, or heat flow, via conduction, to the reservoir is negligible, or too small to be considered.

In the models GLJ has created, as the producer and injector are parallel to each other, a 1D model can be used to understand temperature changes of a fluid flowing through the reservoir. Ideally, the water injected into a formation flows like a perfect piston through the formation, picks up heat uniformly and leaves at the same temperature as the virgin rock. For simplicity, GLJ has assumed that heat transfer within the formation dominates and that conduction of heat into the formation is ignored. Figure 14: Idealized plug flow for EGS modelling. shows this idealized piston model.

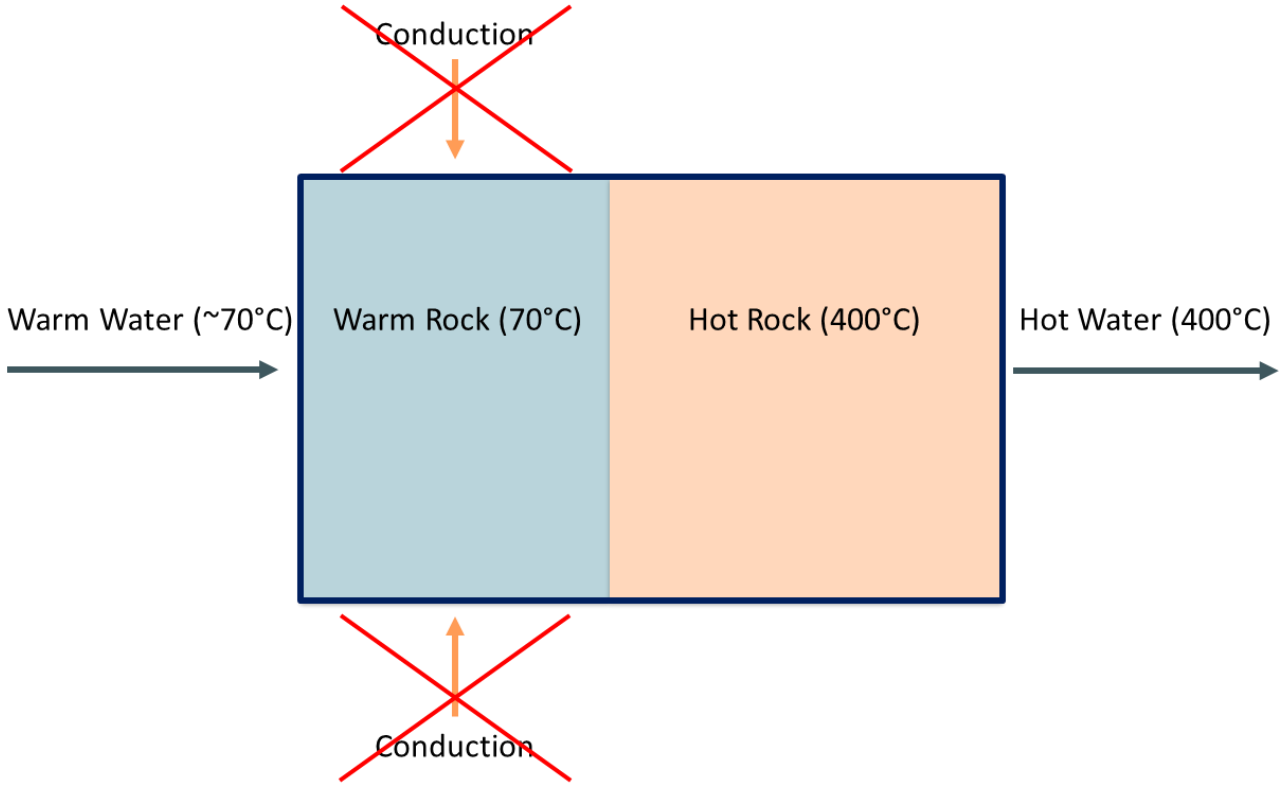

Figure 14: Idealized plug flow for EGS modelling.

However, with real flows, there is dispersion within a formation. This can be due to molecular dispersion, pore-level tortuosity, micro-fingering, fracture flow and conduction of heat from hot to cold fluids. The result is that the flood front will show a gradual change in temperature. How gradual is a key uncertainty and a key reason Monte-Carlo simulation is used for our 1D model.

More specifically, we used a 1D convective-diffusive model. These types of models are well established for flows in porous media and are routinely used in surfactant and solvent flooding applications (initial papers in mid-1950's). These models can simulate changes in both the speed at which the flood front would move through the reservoir and how sharp the front is. It is possible to simulate long-periods of producing high-temperature water, slow changes in water temperature, abrupt changes, and many different pattern sizes. Figure 15: 1D flow with dispersion for EGS modelling. below is an illustration of how dispersion of the cold injected water into the reservoir creates a gradual front rather than an abrupt front.

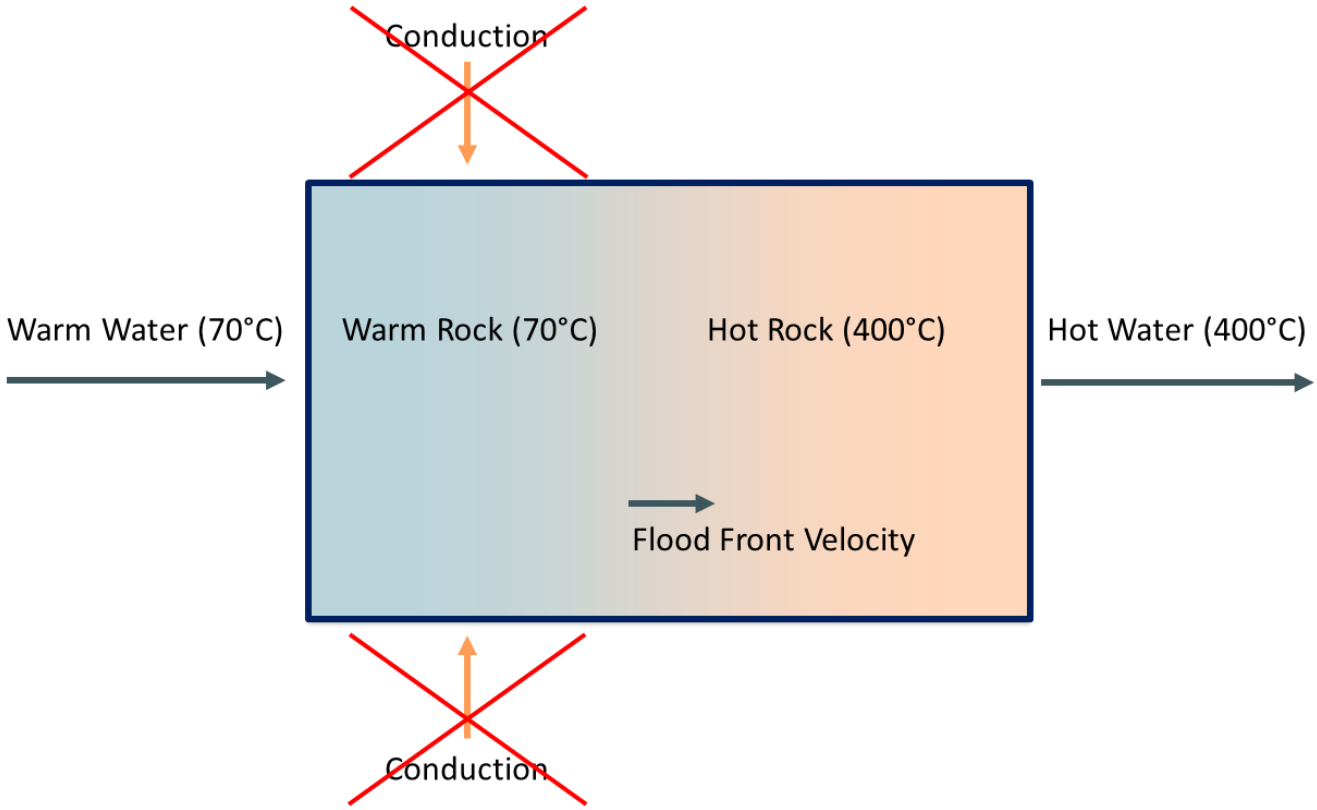

Figure 15: 1D flow with dispersion for EGS modelling.

A further source of complexity comes from real reservoirs being inhomogeneous in both vertical and horizontal dimensions. This results in variable rates of fluid movement at pattern-level scales (i.e., at dimensions of the size of the injector-producer pair). Not all the pore volume will be swept with equal intensity.

Fortunately, with this geothermal process, we have 1) a favourable mobility ratio (M=1), 2) a minimal gravity over/under-ride and 3) a miscible system. These three factors help prevent early breakthrough of injectants and high levels of mixing between injected and native fluid volumes. In other words, these factors help ensure the flood acts like a 1D dispersion problem.

In sedimentary rock with miscible flood for oil, we have observed sweep efficiencies on the order of 40%. Such floods typically use vertical injectors (thus ensuring vertical control of where fluids are injected) on five-spot patterns (allowing areal rebalancing of where fluids are injected). Better control of fluid injection improves sweep efficiency. To be conservative, GLJ further constrained our geothermal model so that the volume of rock swept never exceeds this volumetric sweep efficiency limit. This is an uncertain parameter, so we again used the Monte-Carlo simulation to test how a range of sweep efficiencies would affect the forecasts of produced water temperature.

As hot fluid flows up the vertical section of the producing wells, it leaves the hot reservoir and flows past colder formations and conductive heat transfer occurs. This heat loss is common in geothermal applications and can be calculated using the classical line source model presented by Ramey (1962). Figure 16 below illustrates heat conducting from the wellbore to surrounding rock. Heat losses are highest at early times, slowing over time as the proximal rock heats up. In the figure below, the dark red circle is the wellbore where the larger outer circle with a gradient of red to blue indicate the heat transfer from wellbore to surrounding rock.

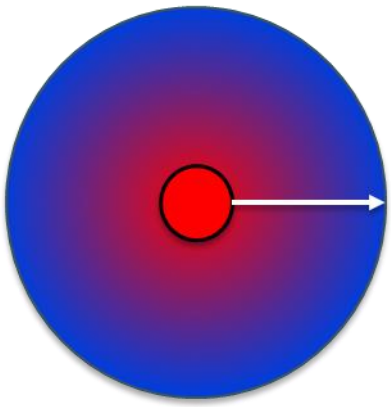

Figure 16: Heat conduction from a wellbore to surrounding cool rock.

Thermal Displacement Modelling – Results

The thermal displacement modelling uses the same inputs as the Heat-in-Place modelling. It is important to note, production modelling results are a model and are to inform the possibility of what a production may look like. Until a well is drilled, tested and on production, thermal modelling is only an estimate.

Table 3: Thermal displacement modelling input parameters and results – High Flow Rate Case.

Inputs	Symbol	Units	P90	Mean	P10
Surface Temperature	T_{surf}	C		60	
Reservoir Temperature	T_0	C		400	
Well Length	m		1000	1250	1500
Distance from Injector to Producer	x	m		500	
Width of Injection	h	m		300	
Number of Injectors				1	
Number of Producers				2	
Sweep Efficiency @ Injector		%	0.3	0.45	0.6
Density of Injection Water	$\rho_{fluid(Inj)}$	Kg/m^3		950	
Density of Reservoir Fluid	$\rho_{fluid(Res)}$	Kg/m^3		750	
Wellhead Fluid Heat Capacity	Cp_f	J/kg*K	2,800	2,900	3,000
Reservoir Fluid Heat Capacity	Cp_f	J/kg*K	2,600	2650	2,700
Density of Rock	ρ_{rock}	Kg/m^3	2700	2800	2900
Rock Heat Capacity	Cp_r	J/kg*K	2,200	2300	2,400
Porosity	ϕ	v/v	0.005	0.0075	0.010
Dispersion Coefficient		m2/s	1.00E-02	5.01E-03	1.00E-05
Full Pattern Injection Rate	Q	bbls/day		100,000	

The dispersion coefficient is the largest degree of uncertainty in the model. High porosity, high permeability or complex fracture growth has low dispersion coefficient whereas large planar fractures in rock would have a relatively high dispersion. The lower the dispersion value, the longer it takes for breakthrough. A range of dispersion values were applied based on assumptions of the type of fractures that can de developed. Complex cloud-fractures in ductile rock would have a relatively low dispersion whereas planar fractures brittle rock would have a high dispersion coefficient.

The thermal recovery factor at 30 years of production was also calculated. The thermal recovery factors range from ~30% which aligns with rule of thumb estimates for conventional doublet designs. Having two methods of calculation which agree gives GLJ more confidence that the results are reasonable.

The temperature profile of the thermal displacement modelling is flat for the first few years as formation water is sweep from the rock then declines as increasing concentrations of less heated injectant are produced. Figure 17: Estimated producer temperature at bottomhole – 100,000bbls/day injection case, given below, displays the estimated temperature as it enters the producer well with a P90-P50-P10 confidence range. P90 refers to a 90% of the calculated values will be equal or exceed P90 estimate where as the P10 values means that 10% of the calculated values will be equal to or exceed this P10 estimate.

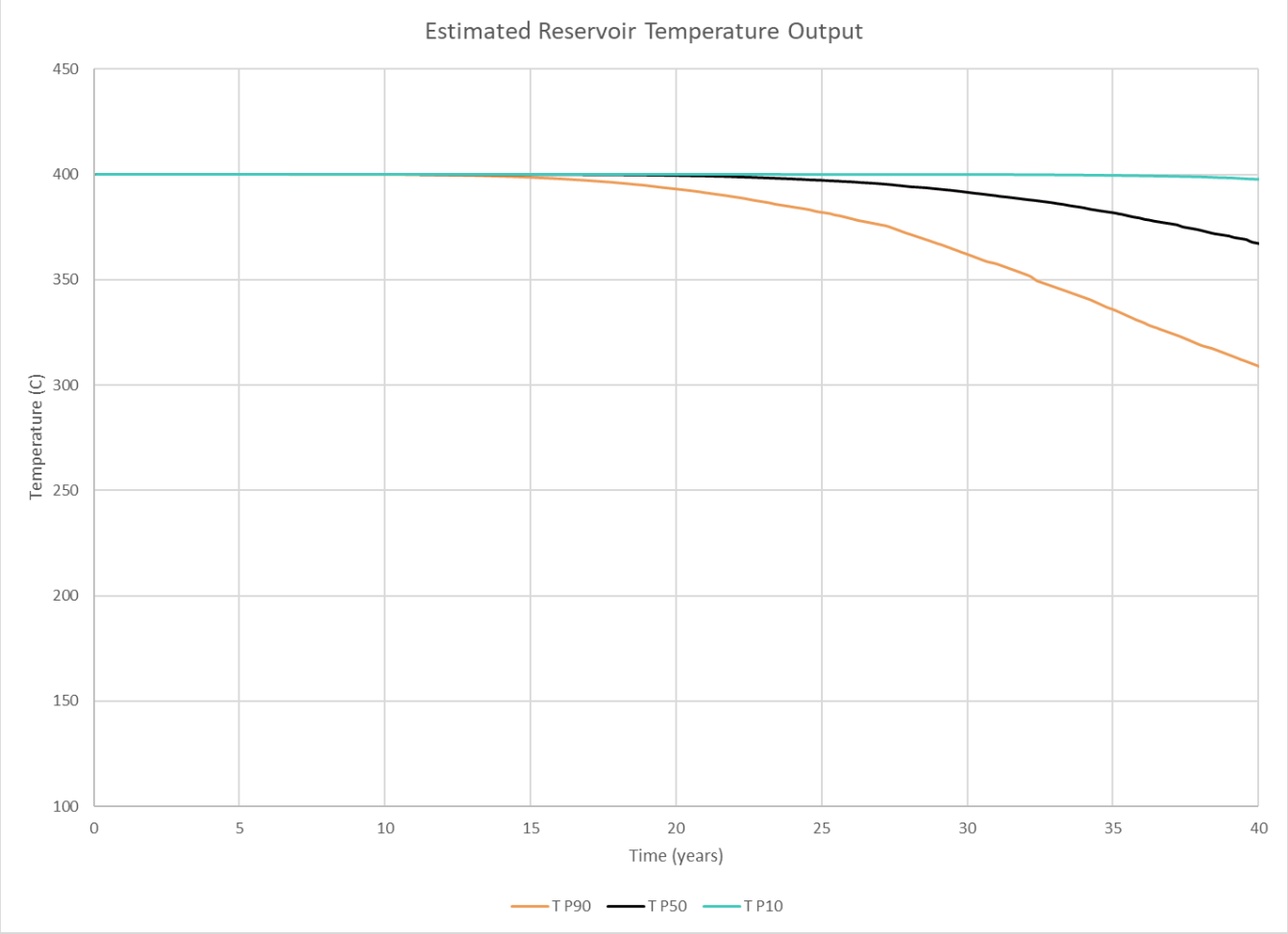

Figure 17: Estimated producer temperature at bottomhole – 100,000bbls/day injection case

The model was then rerun to understand the impact of the spacing between of the wells on the expected output temperature. Runs were completed using well spacing between 50 and 700 metres at 50metre intervals. It was found that 500 metres is the sweet spot for this project with an injection rate of 100,000bbl/day. Below 500 metres the mean modelled temperature drops off too quickly based on a 40-year build life of a facility. At abandonment, geothermal resource would still be left in the ground with a spacing of over 500 metres. With these further distances, there is also potential difficulties for creating a complex fracture network between the wells.

Figure 18: Well spacing sensitivity. Mean temperature shows the mean temperature profiles for the producing well at different spacing.

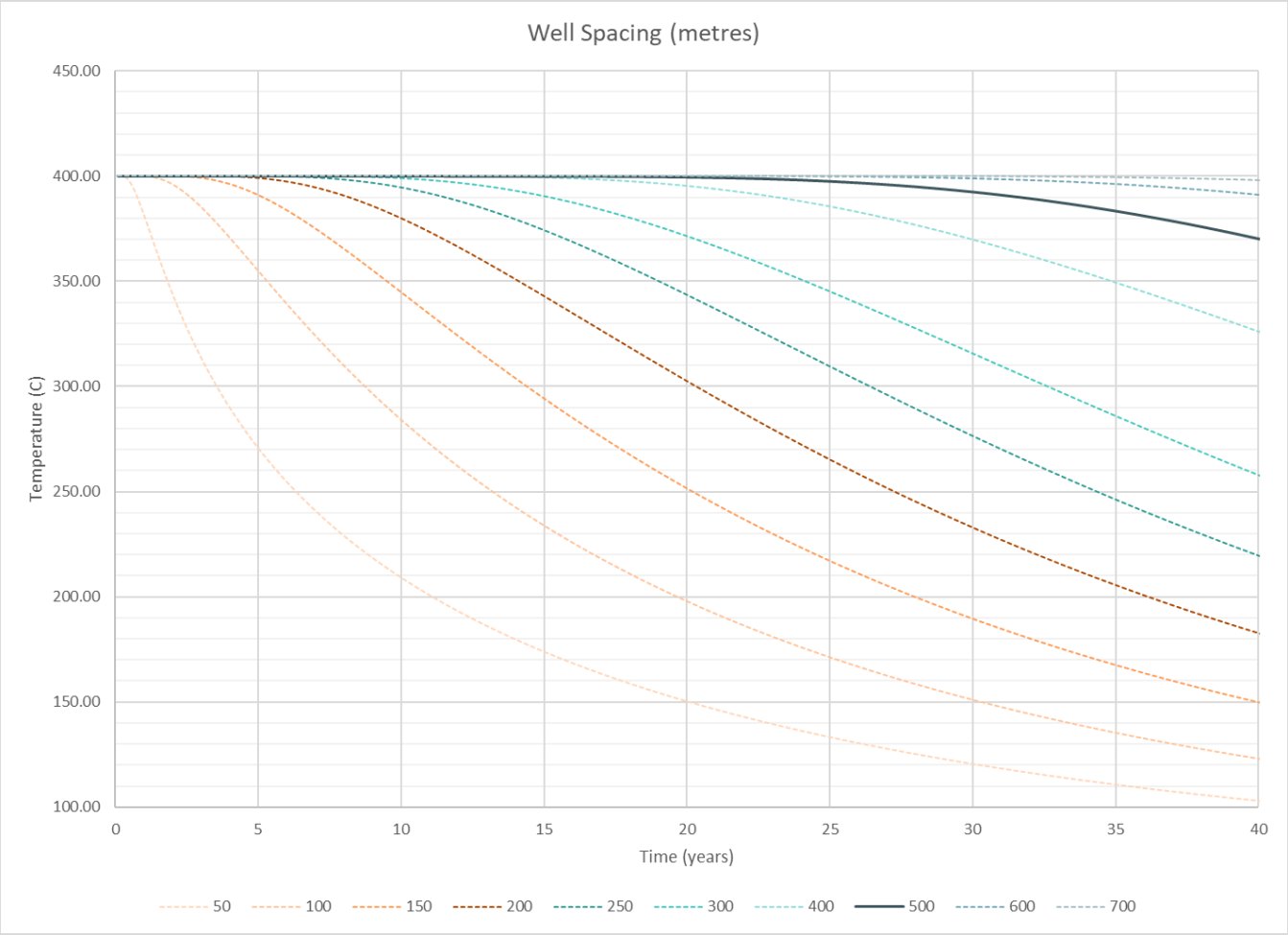

Figure 18: Well spacing sensitivity. Mean temperature at the production well.

With the modelled temperature profile from Figure 17: Estimated producer temperature at bottomhole – 100,000bbls/day injection case, the temperature and flow rate can be used to calculate temperature at surface and the temperature loss in the vertical section of the wellbore as well as include temperature gained while injecting. The temperature loss in the wellbore is about 50°C in the earlier years and decreases to approximately 35°C later in life. In Figure 19: Temperature loss in the vertical section of the production well – 100,000bbls/day injection case below, the blue line indicates the temperature as it enters the production well, where the red line is the estimated temperature at surface.

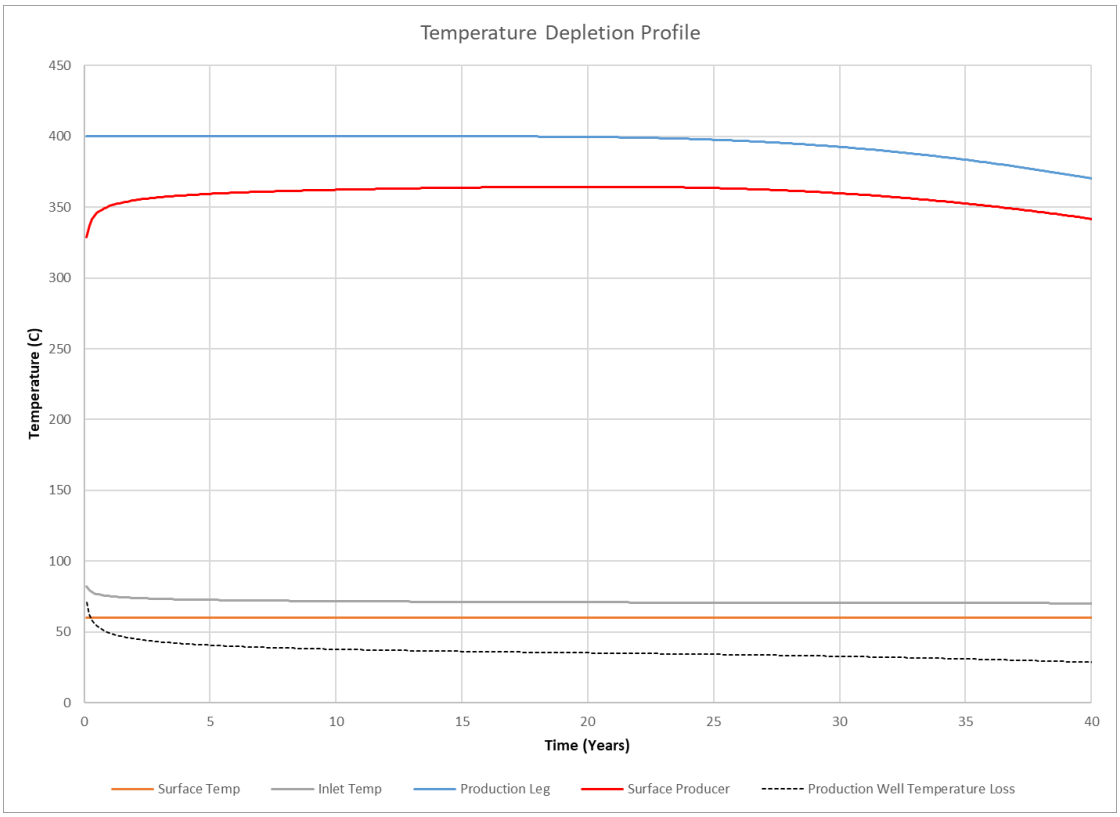

Figure 19: Temperature loss in the vertical section of the production well – 100,000bbls/day injection case

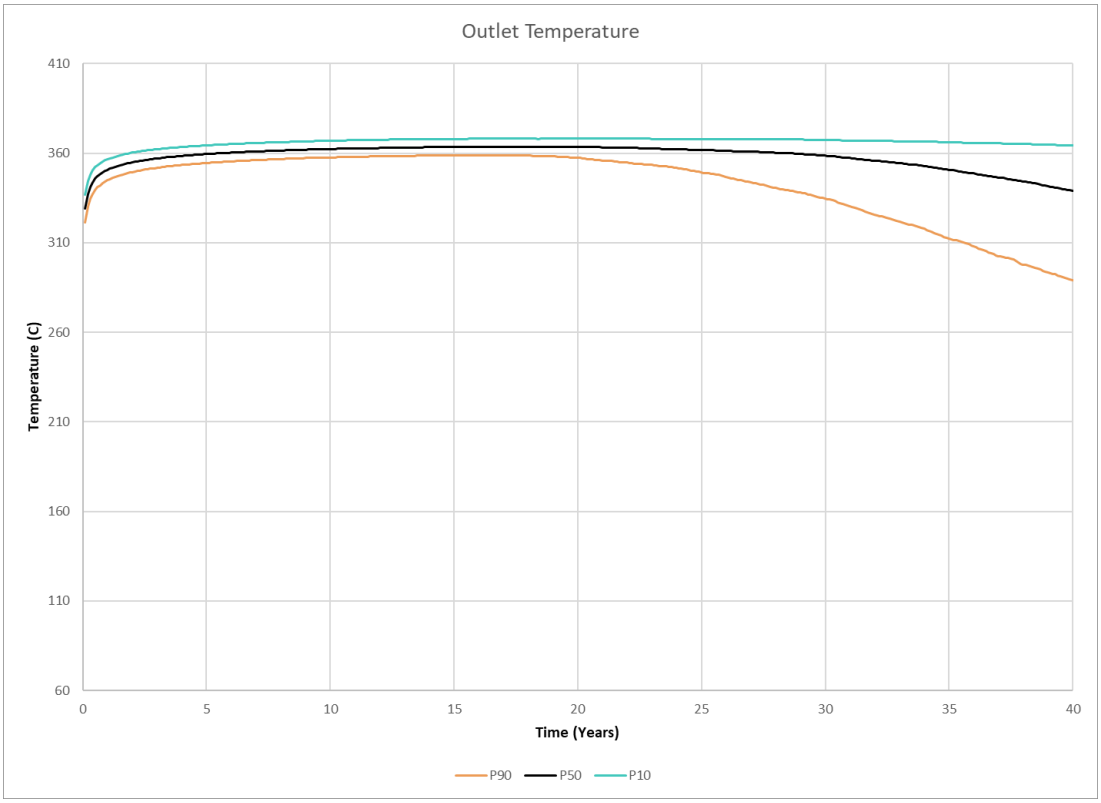

Figure 20: Surface temperature of production wells – 100,000bbls/day injection case

A sensitivity was calculated in which there is a smaller simulated rock volume and as a result, a smaller injection rate. All modelling parameters as above were used except for the distance from injector to producer was adjusted to 300metres and the injection rate was reduced to 50,000bbls/day. The Monte-Carlo Heat-In-Place over a 40-year time frame resulted in a mean value for Gross Wellhead Thermal Energy equated to 31.2MW with the high probability (P90) being at least 25.4MW and the low probability (P10) equating to 37.8MW for the Pad area.

With the reduced area, a reduced injection rate is required of ~50,000bbls/day or a significant temperature decline will occur which will result in depleting the resource before the end of the project life. In addition, as the flow rate is lower, the produced fluids have a longer time in the production well which will result in a higher temperature decrease. Below are a series of model outputs of reservoir temperature, temperature loss in the vertical section as well as estimated temperature at surface for a low flow rate case of 50,000bbls/day. Temperatures at surface are lower in the lower injection case, however the temperatures are still adequate for the surface facilities.

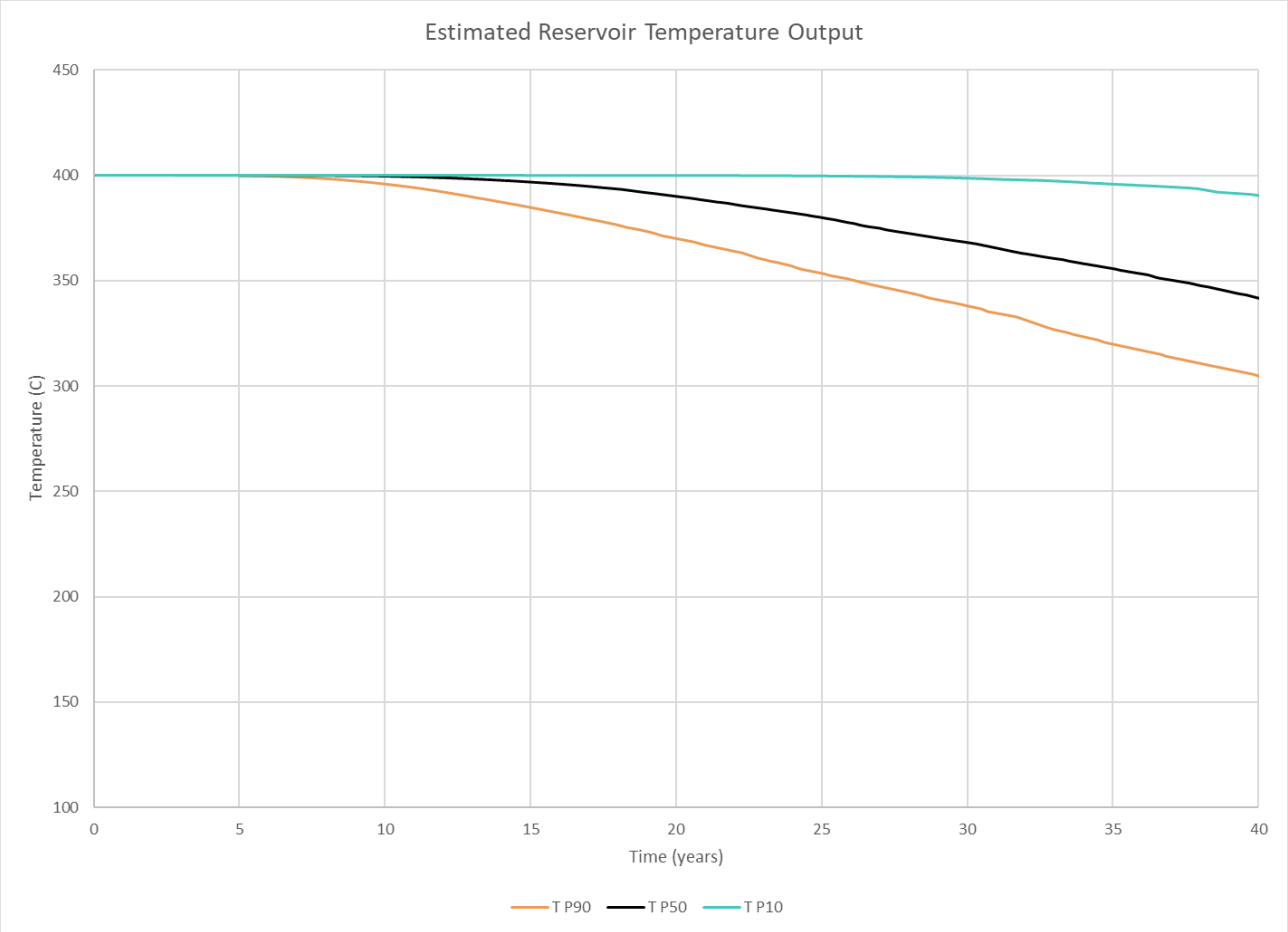

Figure 21: Estimated producer temperature at bottomhole – 50,000bbls/day flow rate case

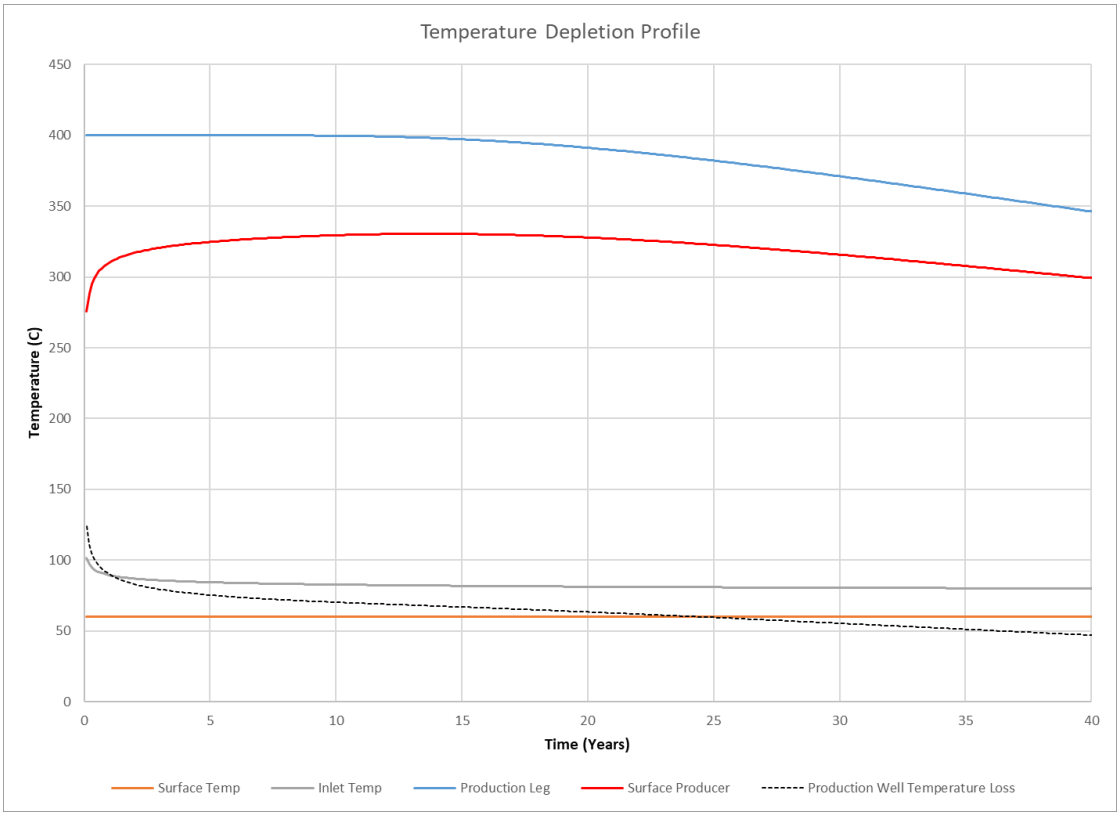

Figure 22: Temperature loss in the vertical section of the production well – 50,000bbls/day injection case

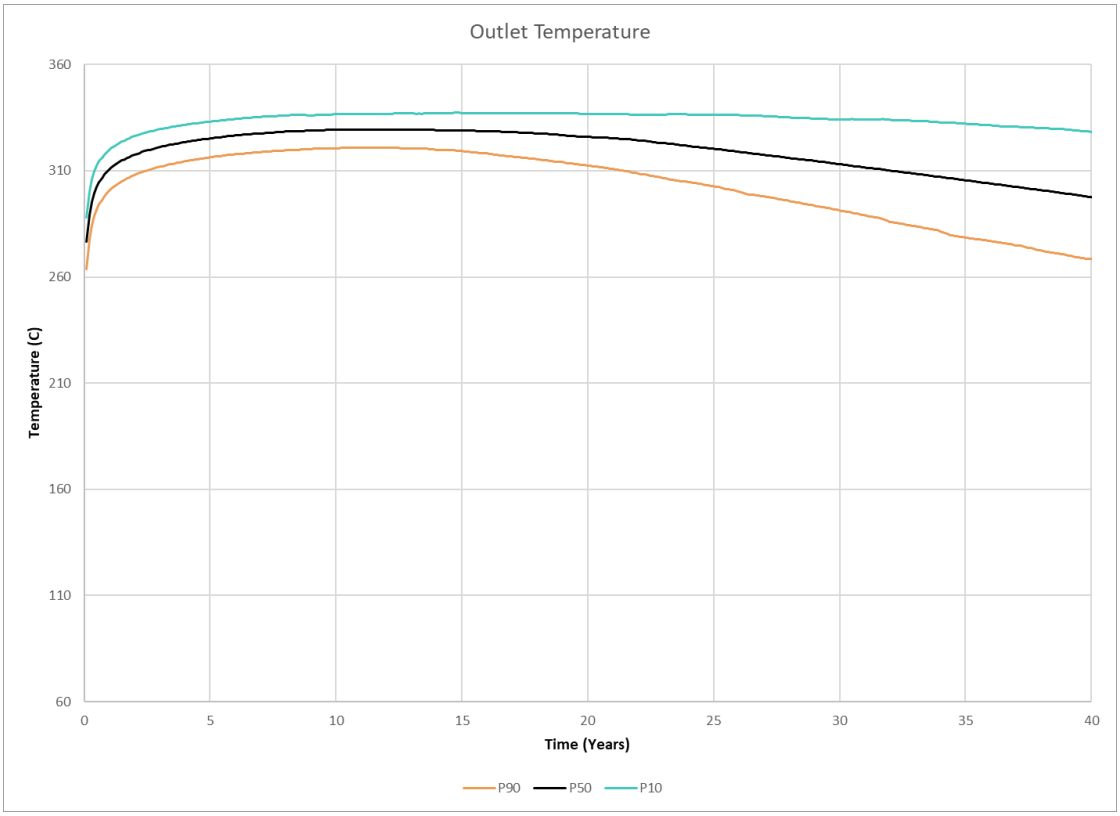

Figure 23: Surface temperature of production wells – 50,000bbls/day injection case

IV. Drilling Review

A 15,000 m vertical depth well drilled through basement rock to 400 °C will be the first of its kind. The closest well to approach that depth terminated 2,700 m earlier. In total 17 wells have been drilled to between 8,000 and 10,000 m TVD and only one went deeper. The situation on the ultra-high temperature side is only slightly better with 28 wells worldwide having exceeded 360 °C downhole temperature. Therefore, given the extremely limited availability of direct offset data, accuracy of the well design, operating parameters, and cost is to be taken as scoping / conceptual.

The conceptual well design presented in this report should be considered extremely leading edge, nearing the point of hypothetical. The risk register contains the known risks and proposes solutions or a path to a solution. While this is necessary to the achievement of any stretch target or goal, it must be realized that the journey to achieve these objectives will certainly be a long one. The past superdeep and ultra-high temperature wells were and are research projects. Technology was and is developed as the wells were drilled to cope with the anticipated conditions.

Despite all best efforts and preparations, success is not guaranteed.

Drilling Review Summary

This report is a research effort to demonstrate the current state of the drilling industry to reach the proposed depth of 15,000 m with 400 °C bottom-hole temperature. Each condition on its own is at the edge of what has been done, however a well with these combined conditions has yet to be drilled. Many of the technical demands have been overcome individually and need to be brought together for this well.

In addition to the drilling risk, there are completion risks related to downhole gauges for temperature and pressure to monitor flow conditions. In the case of hydraulic fracturing, fracture development and permeability will be a serious challenge considering the ductile conditions of the rock at such temperatures.

This well will require an extended period of detailed planning that will necessitate cooperation with the relevant research bodies for ultra-high temperature research projects to learn from their past work. These include but are not necessarily limited to projects in Iceland, Italy, Mexico, and the USA.

Despite the importance of drill bits with regards to progress, the main concern is borehole verticality and integrity. Only a straight hole can be drilled to TD and be completed, otherwise friction will cause drill pipe fatigue due to excessive friction and wear.

High temperature drilling fluids that do not coagulate or evaporate (flash) are required. Control of temperature is key, which is where depth works in the project's favor. Several solutions exist which are likely going to maintain the drilling fluid temperature within the working parameters of available tools.

A detailed geological and geophysical study at the proposed well location is required. This should include deep seismic to establish the location of faults and the brittle-ductile transition zone. Bedding plane position will influence site selection as highly dipping beds should be avoided.

Given the enormous cost and challenges associated with this project, a pilot well to approximately 8,000 m is recommended as a testbed for available and to-be-developed technology. An 8,000 m well has very few peers and will be an indicator if the selected location lends itself to an even more demanding project. A well to 8,000 m will

be a success and can be used for commercial exploitation of a geothermal resource for direct use heat or electricity generation. If such a pilot encounters difficulties beyond repair, the full-scale project will require serious revision.

The costs for so many firsts are going to be high. The presented cost estimate is based on 338 days of operations for a single superdeep well, including completion hardware and installation, as well as 25% NPT for the entire execution phase. This will cost an estimated Cdn $ 101MM. A pilot to 8,000 m can likely be budgeted with Cdn $ 65 MM. Neither well, however, is guaranteed and the cost may double or even triple, without reaching the intended target, as was the case in some of the wells drilled to 10,000 m.

Project details

Project Parameters

The rough terms of reference are outlined in the four bullet points below. What follows is a brief discussion on how they will influence the well design.

- Isolate overburden and prevent groundwater contamination
- 400°C reservoir rock
- 15,000 m vertical depth
- Granite from 750 m TVD overlain by glacial till and other sedimentary formations

Maintaining verticality and borehole stability in a well of this depth into basement will pose a considerable challenge, hence the emphasis on obtaining as detailed a geological survey as possible. This comprises magnetic and gravitational surveys as well as seismic. The chosen site should contain horizontal bedding planes or as close to horizontal as possible and have minimum fractures and faults. This is a finding from the drilling of KTB HB where steeply dipping planes hindered progress and required multiple casing and liner strings. The review of superdeep and ultra-high temperature wells below examines the current experience drilling superdeep and ultra-high temperature wells which provided vital inputs to the proposed conceptual well design and gave confidence to propose the long sections in granite rock.

The ultra-high temperature has a large impact on the well design. While drilling, temperature is maintained in a manageable range, however, during production, the entire well will heat up and likely bring downhole temperatures to surface; like steam injectors but with a flow rate an order or two of magnitude greater than those injectors.

During well construction, rate of penetration is not as important as consistent progress and a quality borehole. Table 8: ROP sensitivity and Table 9: Bit life sensitivityTable 9 include a sensitivity analysis between penetration rate and bit life, and their impact on overall project cost and duration. This highlights that by reducing the number of bit trips, and extending bit life, greater overall savings are realized. Detailed analyses will be required during the detailed planning phase to determine cut-off points and how much ROP can be sacrificed for durability.

Casing material will be selected once detailed simulations are completed and are likely to include corrosion resistant alloys for certain strings or portions of strings, and accessories such as liner hangers, gauge carriers, etc. Rock drillability of a pilot well will have a great impact on the well design. Lessons learned during the pilot well would be indispensable for the design and execution of the 15,000m well. Casing setting depths determine casing exposure to potentially corrosive well fluids and temperature. This in turn impacts material selection, grade, and alloy, making a pilot well the best possible investment.

Wellhead specification will be like steam injectors with regards to tubing hangers and tubing hanger spool. The bulk of the wellhead will resemble a large (476.25 mm / 18 ¾”) deepwater wellhead due to the required capacities

for casing lock down. Work needs to be performed to determine wellhead growth during drilling and production to allow for flexibility.

This leads to soil condition requirements which must be considered when designing the location. The soil around the well will heat up during production and large loads will be transferred to the soil when the production casing is installed.

Conceptual well design is as follows:

Table 4: conceptual well design casing depths

Size	Top (m)	Bottom (m)	Section Length (m)
36 in.	0	150	150
32 in.	0	350	200
26 in.	0	600	250
22 in.	0	1,200	600
14 in.	0	8,000	6,800
9 7/8 in.	7,400	14,000	6,000
8 ½ in. OH	14,000	15,000	1,000

- 36 to 26 in. string isolates the glacial till and upper sediments and provides the needed foundation for the remainder of the well.
- 22 in. casing must be set in the basement rock beyond any potential rubble zone. It can provide a flowpath for injecting cooling fluid into the 14 in. casing.
- 14 in. casing is set at approximately 230 °C, a little more than half-way to TD
- 9 7/8 in. liner is set 1,000 m above TD but is variable depending on progress and completion. It may go all the way to TD if conditions allow and a large, cased hole completion is required.

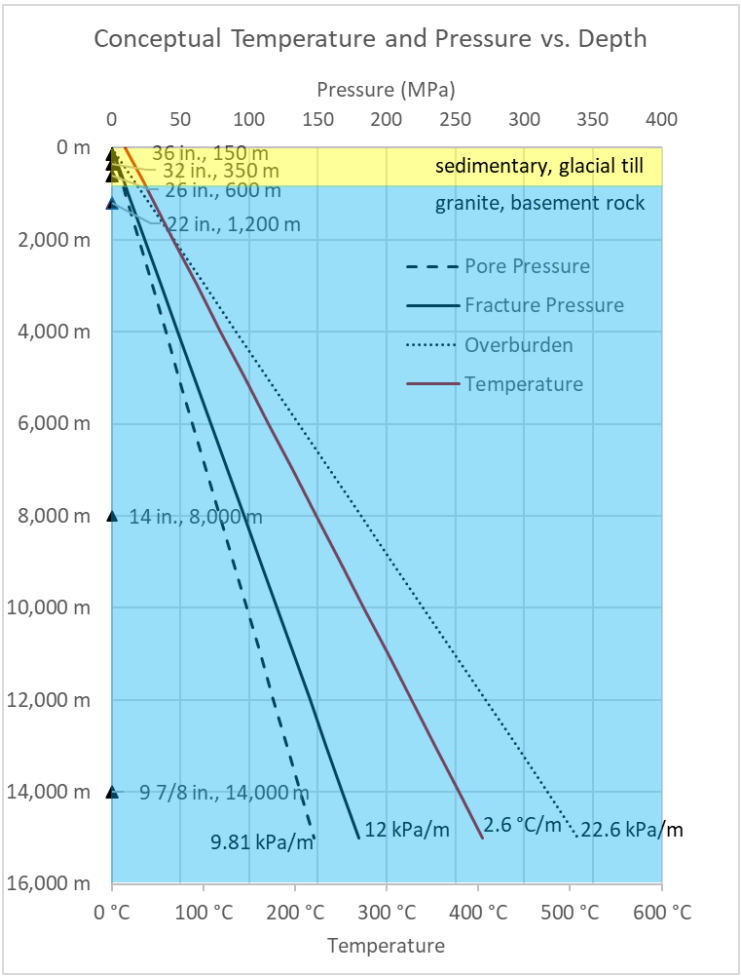

Figure 24: Conceptual temperature & pressure vs. depth

Study Objectives

- Preliminary cost estimate for drilling and completion
- Conceptual well design – schematic only (no detailed casing design)
- Well design parameters for casing and cement, plus completions, and fracturing
- Risk register, analysis, recommendations (high level)
- Review of available and required technologies (high level)
- Completion strategy

The risk register is the main repository of information for the well design and execution as it provides the basis for design questions that must be answered. This is the place where technologies are summarized, and ideas generated.

Production and injection operations

A production scenario with a well pair (injection and production) is one option however, the geomechanics of rock at 15,000 m and 400 °C may not be favorable for such a plan. Several completion and production risks have been identified in the risk register.

Review of Superdeep and Ultra-High Temperature Wells

Superdeep wells are wells of more than 6,000 m vertical depth and have, amongst others, the following features:

- Geological data is predictive, and do not contain a high degree of reliability.
- Design and execution are likely to change as technology develops and geological information becomes available.
- Research and development will continue while drilling to improve operational performance

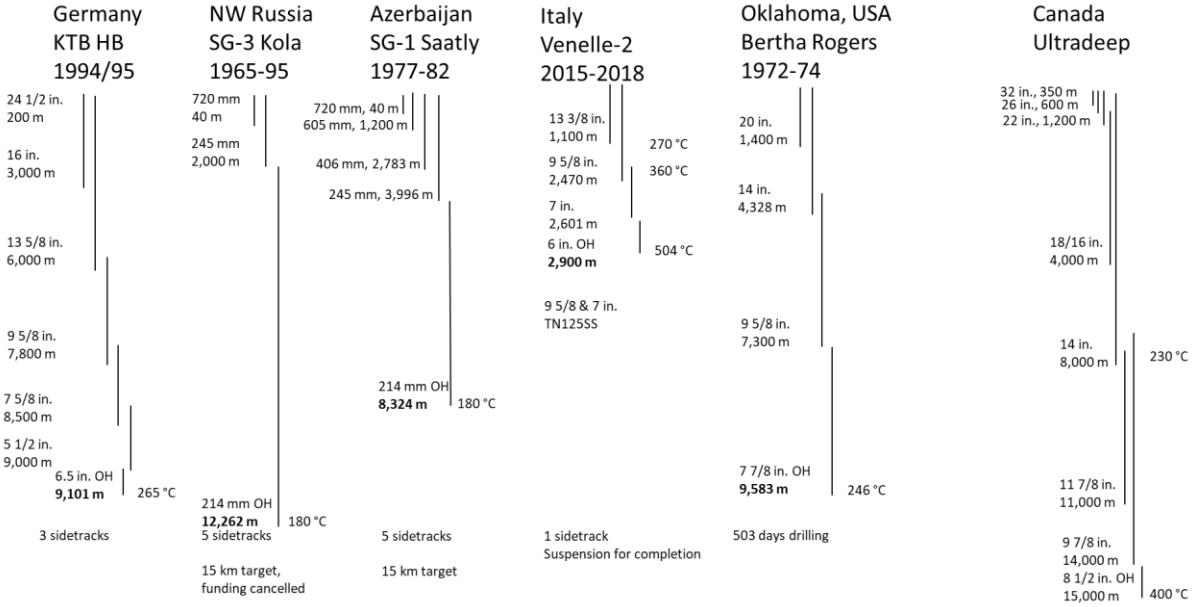

Figure 25: Superdeep and ultra-high temperature known well designs

The schematics in Figure 25: Superdeep and ultra-high temperature known well designs show the known well designs of a few of the deepest wells. Most of the superdeep wells (more on them later) were drilled decades ago and detailed designs are not published or are confidential, as is the case for the BP Tiber and Kakadia wells, and the Chevron #1 well in the USA Gulf of Mexico.

Table 5: Superdeep well objectives below summarizes the known information about the superdeep wells. This is by no means exhaustive as more distinctions are made in the detailed, external, discussions about these wells. There is a multitude of literature available for the KTB project in Germany, as well as Kola SG-3. The Soviet and then Russian superdeep drilling program comprised several wells, but most details are only available in Russian.

Table 5: Superdeep well objectives

Well	KTB	Kola SG-3	Venelle-2	Bertha Rogers
TD	9,101 m	12,262 m	2,900 m	9,583 m
Location	Germany	Kola peninsula Northeastern Russia	Larderello valley Italy	Oklahoma, USA
Objective	Investigate the crustal stressfield, thermal structure of the crust, crustal fluids and transport processes, structure, and evolution of European Variscan basement Remain below 250°C and drill at least 8,000 m	Penetrate the upper crustal layer of granite into the basement rock of basaltic composition	Test geothermal resources at extremely high temperatures for demonstrating novel drilling techniques and control of gas emissions.	Oil and gas exploration
Formations	Gneiss, feldspar, granite	Granite	Volcanic	Sedimentary
Igneous rocks drilled	Yes	Yes	Yes	No, encountered liquid sulphur and abandoned well to 4,000 m.

An effort was made to collect general information on superdeep wells drilled around the world. Table 6 is the result of that research. In total, 18 wells with a TVD of more than 8,000 m have been drilled and of those only one went beyond 12,000 m. No well has ever been drilled to 15,000 m, despite it being the target for two, Kola and Saatly. There are likely additional superdeep wells elsewhere, however, no information is available. An example is a superdeep well in China which is mentioned in research in passing but no well name was shown.

Table 6: Superdeep wells

Wells	Operator	Well name	Spud date	Date compl	County	State	Total Depth (m)	days	Water depth (ft)	Depth from seabed(m)
1	Lone Star Production	#1 Bertha Rogers	11/25/1972	4/18/1974	Washita	Oklahoma	9,583	509		
2	Lone Star Production	#1 Barnest R. Baden	9/4/1970	10/20/1972	Beckham	Oklahoma	9,159	777		
3	Hunt Energy Corporation	1-9 Cerf Ranch	4/29/1979	9/6/1982	Pecos	Texas	9,037	1226		
	Riata Energy	Cerf Ranch		1/1/1994	Pecos	Texas	9,043			
5	Gulf Oil Corporation	2 Emma Lou Unit #1	5/21/1978	7/30/1980	Pecos	Texas	9,029	801		
6	GHK Corporation	#1-34 Duncan	2/20/1981	1/15/1983	Beckham	Oklahoma	8,934	694		
7	GHK Corporation	#1-1 Robinson	7/6/1981	1/25/1984	Beckham	Oklahoma	8,913	933		
8	Chevron USA	#1 University	11/8/1978	6/1/1981	Pecos	Texas	8,762	936		
9	Ralph Lowe Estate	#1-17 University		1/1/1972	Pecos	Texas	8,687			
	Kimball Production	Univeristy #17		1/1/1982	Pecos	Texas	8,687			
10	McCulloch Oil	#1 Easley	4/5/1971	9/18/1973	Washita	Oklahoma	8,245	897		
11	Napeco Inc.	#1 Centurion	10/5/1979	6/23/1981	Pecos	Texas	8,235	627		
	as of February 1985									
	Offshore Gulf of Mexico:									
12	BP	Tiber		2009	Keathley Canyon Block 102	Texas	10,685		4132	9,425
13	BP	Kaskadia		2010	Keathley Canyon Block 292	Texas	9,906		5860	8,120
14	Chevron	Chevron #1		2015	Walker Ridge 758	Louisiana	8,686		6959	*6,565*
					Region	Country				
15	Russian Geological Institute	Saatly SG-1				Azerbaijan	8,324			
16		Kola SG-3			Kola peninsula	Russia	12,262			
17		Tymen SG-6			Siberia	Russia	*7,502*			
18		En-Yakhin SG-7		2000	Novy-Urengoy	Russia	8,250			
19		West Aladag-1 (AZ)				Azerbaijan	9,620			
20	Germany, Kontinentale Tiefbohrung	KTB HB		1995		Germany	9,101			

Ultra-high temperature wells have downhole temperatures of more than 205 °C, in oil and gas terms. In the geothermal industry, wells with more than 374 °C downhole temperature are referred to as super hot rock systems (SHR) as water is supercritical at temperatures above 374 °C. The wells drilled for the purpose of exploiting this temperature are generally less than 5,000 m, and in most cases less than 3,000 m deep.

Geothermal wells with a bottom hole temperature 400 °C or higher have been completed in several areas around the globe as shown in Table 7. The expertise varies, and research is on-going to develop the resource, albeit at a third of the proposed well depth. The table below shows the wells that have exceeded the critical temperature of 374 °C.

Table 7: Ultra-high temperature wells

Wells	Country	Region	Well	Depth	Temperature
1	Italy	Larderello	Sasso 22	4,092 m	380°C
2		Larderello	San Pompeo 2	2,966 m	400°C
3		Larderello	Venelle 2	2,900 m	504°C
4		Larderello	Carboli 11	3,455 m	427°C
5		Mofete	San Vito 1	3,045 m	419°C
6	Iceland	Hengill volcano	NJ-11	2,265 m	380°C
7		Reykjanes	RN-17	3,082 m	320-380°C
8		Krafla	IDDP-1	2,104 m	450°C
9		Krafla	K-36	2,501 m	380°C
10		Suðurhlíðar	K-39	2,865 m	386°C
11		Reykjanes	IDDP-2	4,659 m	427°C
12	Japan	NE Honshu	Kakkonda WD-1a	3,729 m	500°C
13	USA	The Geysers	Wilson No.1	3,672 m	400°C
14		The Geysers	Prati-32	3,396 m	400°C
15		Salton Sea	IID-14	2,073 m	390°C
16		Puna Hawaii	KS-2	2,440 m	342°C
17		Puna Hawaii	KS-13	2,488 m	1,050°C
18		Puulena Hawaii	Lanupuna-1	2,557 m	363°C
19	Mexico	Los Humeros	H-8	2,300 m	380°C
20		Los Humeros	H-11	2,376 m	380°C
21		Los Humeros	H-12	2,984 m	380°C
22		Los Humeros	H-26	2,546 m	380°C
23		Los Humeros	H-27	2,584 m	380°C
24		Los Humeros	H-29	2,186 m	380°C
25		Los Humeros	H-32	2,186 m	380°C
26	Kenya	Menengai	MW-01	2,198 m	391°C
27		Menengai	MW-02	2,118 m	390°C
28		Menengai	MW-06	2,172 m	325°C

Conceptual Drilling Cost Estimate

A conceptual drill cost estimate to calculate drill cost for a single well was completed to assist with economic calculations. Below is the Time & Cost vs Depth curves and the assumptions which went into this estimate.

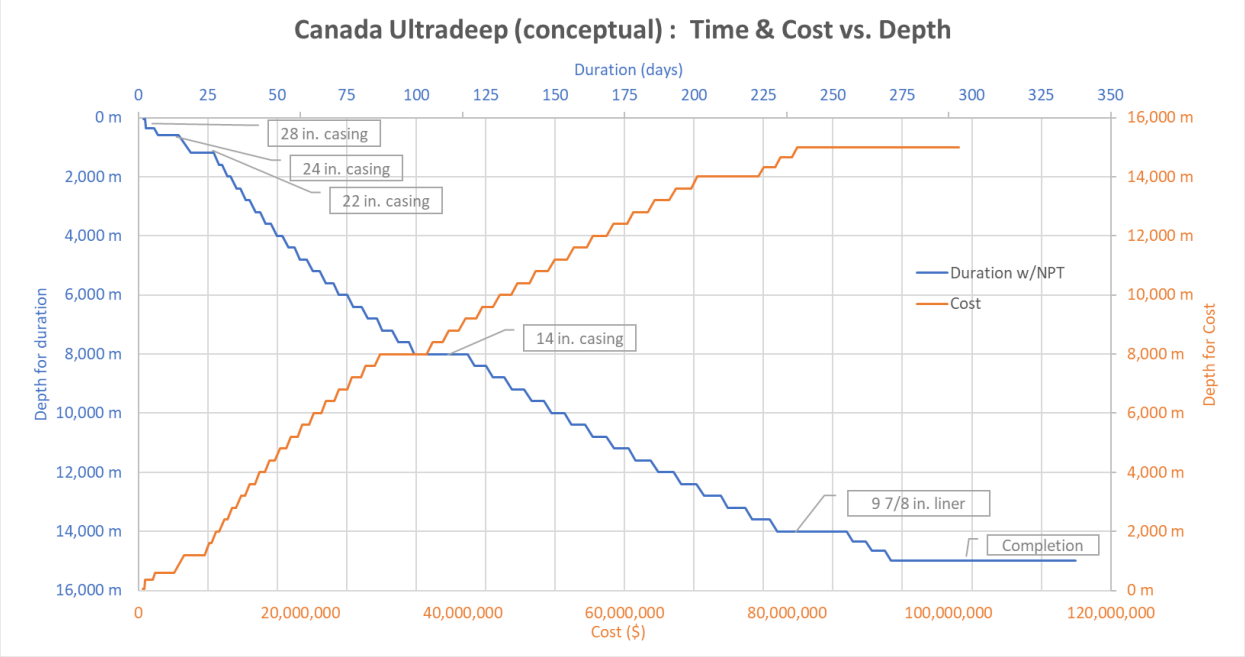

Figure 26: Drilling Time & Cost vs. Depth

Assumptions:

- The accuracy of this estimate is purely qualitative and assumes optimistic progress without any major complications. The cost could easily double, or even triple if serious problems arise such as unexpected rock behavior, borehole stability due to bedding planes, etc. Although the cost may be slightly less due to better-than-expected progress, more resilient materials, etc. The probability is considered low.
- A 25% contingency (time and cost), in addition to the presented estimate is prudent
- Drilling and completion costs are considered all-in, including extra standby equipment such as mud coolers, pumps, MPD, etc.
- No contingency string (18, 16, 11 7/8, or 7 in.) cost has been included
- 42 days completion @ 300k $/day included for services and equipment
- Cdn $ 300,000/day all-in rate (Cdn $ 101.3 MM)
- 25% NPT included

Sensitivities:

- Completion program to be developed

Table 8: ROP sensitivity

ROP (m/hr) base case (BC): ≥17 1/2 in. section: 10 m/hr, ≤12 1/4 in. section: 7.5 m/hr				
≥17 1/2 in. section	5	10 (BC)	15	20
≤12 1/4 in. section	5	7.5 (BC)	10	15
Duration (days)	400 (+63)	337	313 (-24)	294 (-43)
Cost estimate (mln$)	120.1 (+18.8)	101.3	93.8 (-7.5)	88.3 (-13.0)

Cost change with improved or reduced bit life expressed in bit trips. Base case is 400 m/bit.

Table 9: Bit life sensitivity

Bit life – base case ROPs, only change one section bit life at a time			
17 1/2 in. section	283 m/bit, 24 bit trips	400 m/bit, 17 bit trips (BC)	680 m/bit, 10 bit trips
Duration (days)	354 (+17)	337	321 (-16)
Cost estimate (mln$)	106.3 (+5.0)	101.3	96.2 (-5.1)
12 1/4 in. section	300 m/bit, 20 bit trips	400 m/bit, 15 bit trips	600 m/bit, 10 bit trips
Duration (days)	363 (+26)	337	312 (-25)
Cost estimate (mln$)	108.9 (+7.6)	101.3	93.6 (-7.7)

High-level Risk Register

The review of existing superdeep, and ultra-high temperature wells demonstrates the limited industry experience. As the development of geothermal resources continues, so does the search for solutions to current problems related to temperature. Several regional and international research bodies are dedicated to the improvement and development of new materials to reduce temperature-related issues. Ultra-high temperature related issues in electronics and material can be mitigated by continuously circulating a cooling fluid and new materials for computer boards that can withstand these temperatures. This will potentially help resolve borehole-related issues by allowing logging-while-drilling tools to be used as well as rotary steerable systems.

The following research institutes have been working in geothermal resource development projects:

- SINTEF Energy Research, Trondheim, Norway
- KMT (Krafla Magma Testbed), Iceland
- DEEPEGS (Deployment of Deep Enhanced Geothermal Systems for Sustainable Energy Business), Iceland
- DESCRAMBLE (Drilling in dEep, Super-Critical AMBient of continental Europe), Larderello, Italy
- GEMex (Europe-Mexico project), Los Humeros, Mexico
- HADES (Hotter and Deeper), Taupo Volcanic Zone, New Zealand
- IDDP (Icelandic Deep Drilling Project), Iceland
- JBBP (Japan Beyond Brittle Project, drill past the brittle-ductile boundary into 500°C systems), Japan
- NDDP (Newberry Deep Drilling Project, drill past the brittle-ductile boundary in Newberry volcano), USA
- HiTI project (High Temperature Instruments for supercritical geothermal reservoir characterization and exploitation)
- IMAGE (Integrated Methods for Advanced Geothermal Exploration) initiative
- US DOE Frontier Observatory for Research in Geothermal Energy (FORGE), USA

The following is a high-level summary of risks that can be expected while drilling. Table 10: Drilling Risk risk register, which is based primarily on experiences that were encountered in the superdeep and ultra-hot wells drilled to date, is not exhaustive, and would need to be revisited should the project progress to the next stage of planning. The solution-column contains one of two qualifiers: evolutionary (E) or revolutionary (R). “Evolutionary” is an improvement of existing technology such as insulation of tools, performance testing of exiting tubular connections, etc. “Revolutionary” are developments such as new ultra-high temperature-withstanding electronic components using silicon carbide CMOS technology, or never used drilling fluid additives. These solutions have not been studied and could therefore introduce other unforeseen challenges and risks.

Table 10: Drilling Risk Register

Item	Risk	Challenges	Solution	Impact on success
	DRILLING			
1.1	HSE	Handling hot fluids and equipment on surface. Drill floor enclosure to avoid people in the hot zone.	(E) Automated, remotely operated equipment, robotics, remotely operated valves, equipment redundancy to allow working on cooled-down equipment.	Crucial to develop working methods and conditions.
1.2	Insufficient tubular capacity due to hole depth and geometry limitations	Material performance, tensile strength	(E) Higher grades, improved connections	Existing technology allows reaching of the project depth. Depending on the conditions (acidic environment, etc.) present in the well, equipment capacities may be reduced.
1.3	Drilling fluid deterioration	Decomposition under temperature Coagulation leading to plugging	(E), (R) Water, high temperature polymers to maintain solids in suspension	Existing technology allows drilling at 400+°C e.g., Iceland, Italy
1.4	Pore pressure (unexpectedly high)	High pore pressure, unexpected connection to high pressure "bubbles" via faults and fractures	(E) LWD (to a certain temperature limit) pore pressure prediction	Unforeseen pressure, in combination with corrosive fluids and high temperature can jeopardize the well
1.5	Bits	Durability ROP	(E) PDC, air hammer if dry granite, air drilling/foam/mist if dry rock as much as possible, particle drilling (revolution)	Slow ROP or several bit changes can negatively impact hole conditions, also more work by rig equipment, etc.
1.6	Casing – corrosive fluids	Lifting of downhole, native, fluids to surface that are likely to contain brines (highly saline), gases (CO2, H2S, CH4), potentially acids (HCl, HF, etc.)	(E) maintain non-corrosive environment through injection of neutralizing chemicals, maintain temperature and pressure to reduce or eliminate corrosion, use CRA	Depends on material selection: minor to major impact related to cost
1.7	Casing thread compound		(E) Solid dope, pre-doped Clean well/Dopeless pipe (evolution)	Already in use, no negative impact
1.8	Casing sealing mechanism under high temperature	High tensile load	(E) Tubular providers work to qualify connections and provide installation procedures.	Already developed and in use
1.9	Casing – collapse	During drilling and production, fluid expansion may excessive external casing loads. Production of steam/blow-down of transport tube or annulus can expose casing	(E) preliminary engineering can identify problem situations. Engineering controls such as annular flooding can ensure fluid level to prevent catastrophic failures.	Crucial to consider all drilling, completion, stimulation, production scenarios to simulate well conditions and select best strategy.

Item	Risk	Challenges	Solution	Impact on success
		and/or tubing to high differential pressures.	(R) Electronics are required for precise measurements of downhole conditions to allow controls to be activated.	
1.10	Cementation of casing	Achieve durable solid cementation of casing and liner. Retardation in high temp environment with long pumping times due to well depth. Setting-time extension for deep and hole wells due to extended placement time.	(E) Evolution of existing cements with suitable additives. Halliburton ThermaLock™ (R) Development of new materials or combinations that set up under great temperatures or remain flexible yet maintain a seal and pressure integrity, or materials that are set off by a trigger and melt in place, like bismuth plugs, heat-resistant expandable foams pre-molded to casing, etc.	Cement formulation (Halliburton ThermaLock™) already available, application at these depths has not been done.
1.11	Cement for sidetrack kick-off plugs		Halliburton ThermaLock™	Cement already available, application at these depths has not been done.
1.12	Borehole stability (squeezing formations)	Maintain sufficient wellbore stability at depth with potential losses into faults and gains from faults and fractures of unknown density and pressure. Rubble zones around faults and brittle zone are likely areas of instability.	(E), (R) Casing off trouble areas, however insufficient string available and underreaming high UCS rock should be avoided (see "offsets"). Investigate alternative hole stabilization methods. MetalSkin™ by Wfd for open hole expandable technology	Great impact on reaching TD.
1.13	Mud cooling	Injection of cold mud into annulus (recognising kicks, losses), surface cooling	(E) higher efficiency mud coolers, cooling technology to reduce injection temperature close to freezing. Entire cooling chain on surface.	A make-it or break-it technology. Available and backups are required.
1.14	Drilling with/maintaining fluid under pressure	RCD (RCD rating pressure and temperature) Water will be supercritical at ~8,000 m → 14 in. casing point	(E) improvement of existing technology to deal with higher temperatures such as internal cooling of components (R) Development of new ultra-high temperature sealing elements. New valve technology and design	Major

Item	Risk	Challenges	Solution	Impact on success
1.15	Verticality – directional control	The hole must be as vertical as possible to minimize friction and drag	(E) RSS to about <8,000 m, then motor drilling with limit MWD, maybe pump down wireline surveys (R) new drilling concepts for 8,000+ m) Most likely evolutionary with more heat resistant materials and cooling.	HT RSS can be used until it gets too hot. Continuous circulation can help to reduce tool temperature in conjunction with very efficient surface mud coolers
1.16	Downhole electronics	Current technology can maintain electronics working at 300-350 °C for a certain amount of time, not indefinite.	Temperature and pressure are in combination are the greatest challenge to electronics. (E) Cooling with dry ice at surface. (R) New tools being developed by projects such as SINTEF, HiTI, GeoWells, IMAGE, etc. using new electronic component materials	Important for logging and MWD when circulation is interrupted for longer periods.
1.17	Rig capacity	Hookload: Large string weights for 14 in. intermediate casing. Torque capacity	(E) Custom rig design and specs (1,400 kdaN hook load, 40-m stands, etc.)	Major
1.18	Research aims	Determine what is required (full size core, sidewall core, cuttings (simple), fluid samples (wireline logging), etc.)	Depending on the required parameters, tool availability can be confirmed with the relevant research institute.	Tool application must weigh against risk to achieving the well objectives.
1.19	Continuous circulation	Maintain downhole cool to ensure working conditions.	Provides continuous cooling to downhole tools.	Key to success
1.20	Fluid influx at faults	Composition (highly saline/saturated brine with dissolved gases: CO_2, H_2S, H_2, CH_4), temperature, pressure	Fluid influx can be measured best with quantitative flowmeters such as Coriolis f mass flow meters installed in the return lines, ideally as part of an MPD installation.	Can be great if it is the wrong combination and requires extensive remediation work up to casing or liner running (see offset).
1.21	Wellhead	Pressure & temperature rating and material for corrosive fluids	(E) Available in the offshore market, can be adapted to onshore.	Minor
1.22	Liner hanger, running tool rating	623 kdaN 9 7/8 in. liner weight to be suspended from 14 in. casing	(E) the equipment exists for deep offshore wells; however, temperature qualification must be performed. This is true for most downhole tools.	Minor, optimize well design to accommodate technology, develop better technology.
1.23	Surface equipment	Pumping hot fluids for long periods will affect pump parts, hoses, valves	(E) Mud cooling; simple solutions are available but need to be redundant.	Major

Item	Risk	Challenges	Solution	Impact on success
	durability and reliability		Annular injection of cool liquids.	
1.24	Equipment breakdown	Require redundancy on surface to ensure continuous circulation	(E) employ redundancy, alternative sources	Major if cooling is lost and downhole tools are cooked to destruction.
1.25	Wireline tool and wire	Potential hydrogen embrittlement of electric and slickline cables, also high pressure, and high temperature grease for cables	(E) Materials are available at a cost. Main requirement are temperature and pressure gauges along the length of the well.	Minor
1.26	Recovery from stuck pipe incidents at depth	The great temperature and long run-in times with wireline have in the past led to the decomposition of explosives in string charges. Due to the small diameter, insulation of the explosives is nearly impossible.	Design weak points into the drill string which brings other risks. Mechanical cutters, they may be designed for drill pipe or drill pipe with sufficient ID must be used.	Major

Advanced Drilling Technologies

New drilling technologies are be developed to increase bit life as well as rate of penetration thus in turn would decrease well costs. These new technologies are still in their infancy and have many hurdles to overcome until the technology is commercial. However, there has been recent success with PDC drill bits in granite from the drilling at the Utah FORGE project.

Upcoming geothermal drilling technologies include:

- Particle Impact Drilling
- GA Drilling's PlasmaBit drilling technology
- Quaise millimeter wave (MMW) drilling technology

V. Facilities Overview

COSIA is considering the use of a heat recovery circuit for deep geothermal fluids as a sustainable replacement for OTSGs with which to create steam from boiler feed water (BFW). To provide sufficient thermal energy, there will be several production and injection wells to circulate water through an open loop in the rock formation and re-heat the fluid.

Two different methodologies were reviewed for utilization of the thermal energy: a non-flashing and a flashing case.

In our view, these cases represent two different surface facility design possibilities. The non-flashing case represents the simplest exploitation of the concept in which geothermal fluid is directly exchanged as a high temperature liquid to supply heat in water-heat boilers as a replacement for OTSGs. As such it is the simplest, lowest scope to use geothermal heat with all other components of the SAGD facility remaining the same. The flashing scenario provides an early view to a concept where sufficient heat is used to perform OTSG heat replacement and to generate more than sufficient power to offset the electrical power used by the SAGD site.

The non-flashing scenario requires less processing equipment resulting in a lower capital cost but does not capture the full potential of the energy available for use. The flashing scenario requires great capital investment. Both the flashing and non-flashing cases have further room for study and optimization, but high-level results are outlined below.

Facility Design Basis and Assumptions

The overall facility design is based on the following basis and assumptions:

- Each geothermal well is approximately 15 km deep.
- Operating conditions within the geothermal well are ~ 400°C and 150 MPa with starting enthalpy at 1777.3 kJ/kg.
- Rock formation is hot and dry.
- An open loop through the rock allows for the injected fluid to re-heat in the formation.
- 6 geothermal producer wells and 3 geothermal injector wells are connected to the facility via surface pipelines. Each well is assumed to be within 2 km of the SAGD CPF.
- A separate power generation area of the plant is required for the flashing scenario only.
- Overall flow rate and the number of deep wells required for production and injection are not a design limitation.
- Geothermal reservoir can provide continuous heat to the geothermal fluid for the life of the facility.
- Produced geothermal fluids contain minimal to no dissolved gases, but potentially have substantial dissolved ions.
- NORMS (naturally occurring radioactive materials) are not present in these dissolved ions.
- Geothermal fluid temperature for cross exchange with the BFW is ~ 350°C.
- Temperature of the geothermal fluids for re-injection ~ 200°C.
- BFW inlet to the cross exchanger is 163°C and 800 m^3/h, with an outlet temperature of 310°C and 90% steam.
- 343 MW of thermal energy is required to heat the BFW to replace the OTSGs that would be used in a traditional setting.

Process Flow for the Non-Flashing Scenario

A sketch of the non-flashing block flow diagram with a heat and material balance is included in the Appendix for reference, noting that within this case, the geothermal fluid will remain as a liquid from production wellheads through to injection wellheads.

The BFW inlet cross exchanges through multiple waste-heat boilers (exchangers with steam separators and preheaters) with the geothermal fluid to meet the desired BFW criteria of 90% steam at 310°C. After cross exchange with the BFW, a slip stream of 5% of the geothermal thermal fluid is removed as blowdown and is sent for disposal to reduce the ionic buildup in the water. Make-up water is added to maintain the geothermal fluid circulation flow rate constant. The remaining geothermal fluid with the make-up water is sent for conditioning and is then pumped into an injection well to complete the thermal circulation loop.

Process Flow for the Flashing Scenario

A sketch of the flashing block flow diagram with a heat and material balance is included in Appendix B for reference, noting that within this case, the geothermal fluid is flashed to further capitalize on the thermal energy available. The entire geothermal stream is flashed at 13.4 MPa to obtain a flashed steam for OTSG replacement and the liquids for further use in power generation and heat optimization.

Geothermal fluid flows from the producer gathering network into the SAGD plant geothermal inlet at high pressure and temperature. After the inlet the entire geothermal fluid is reduced in pressure to 13.4 MPa where it is directed into several flash vessels, flashing about 20% of the stream. The flash steam is used for SAGD BFW evaporation. The geothermal condensate is separated and sent to the LP Steam and Power Generation Unit where the pressure is reduced further, creating additional steam at 3.5 MPa. The 3.5 MPa steam is utilized to create approximately 150 MW of power. The power, which creates minimal emissions and is a sustainable, renewable source of power, can be utilized within the facility to minimize operational costs as well as provide a positive impact on total facility emissions.

The power generators are driven by condensing turbines using all the 3.5 MPa steam for power. The remaining geothermal condensate is utilized in various heat exchangers to optimize heat recovery and including SAGD BFW preheat, turbine superheat and reheat.

A slip stream of 5% of the geothermal thermal liquid is removed as blowdown from the LP Steam and Power Generation Unit and is sent for disposal to reduce the ionic buildup in the water. The remaining 95% of the geothermal liquid is gathered, co-mingled with the 5% make-up water, conditioned, and pumped into an injection well to complete the thermal circulation loop.

Technical Uncertainties

Several major uncertainties exist for these concepts:

1. Reservoir enthalpy: Based on anticipated subsurface conditions in the hot rock, an enthalpy of 1777.3 kJ/kg was used. However, no drilling has been done and no actual enthalpies were used in the creation of this report.
2. Surface enthalpy: Losses of enthalpy are unknown. However, once thermal wells operate for long periods of time thermal losses reduce as the near-well-bore area heats. For the purposes of this report, no loss of enthalpy was used to compound on the existing reservoir uncertainty. The 1777.3 kJ/kg starting enthalpy was used at surface.
3. Well layout: Such a project has not been constructed before. No surface locations are defined and no well site layouts are available to use. Distances from plant are arbitrary only.

4. Geothermal fluid analysis: It is fully expected that dissolved solids will be present in the producer wells and that a continuous blowdown and make-up will be required. While it is expected that 5% of the total flow for blowdown will be sufficient, there is no evidence that this is either too large or too small. Many ions may be present, and some may require treatment in the blowdown prior to disposal. However, no costs for such treatment are included as it is not demonstrated necessary. Fouling factors to compensate for TDS induced scale or corrosion are included but many be insufficient.
5. Naturally Occurring Radioactive Materials (NORMS): Deep subsurface water can contain NORMS. Within reason, this may not affect the facility CAPEX, at end of life, materials that have become radioactive because of contact with such water will have additional reclamation costs.

Geothermal Pipeline Networks

Production and injection networks are required for geothermal fluids. Assumed production and injection pressures are 25 MPa with high production temperatures. All geothermal pipelines are surface located on piles with insulation to minimize thermal losses. Each production well is forecast to flow 331 m3/h and injection wells forecast to receive 662 m3/h in a high injection rate case. The non-flashing case is projected to use 6 producers and 3 injectors. The flashing case is projected to use 14 producers and 7 injectors.

Facilities Discussion

The following table outlines the differences between the non-flashing and the flashing scenarios.

Table 11: Facility Design Criteria

Criteria	Non-Flashing Scenario	Flashing Scenario
Water Use	1,336 Ton/h	3,398 Ton/h
Production Well Count	6	14
Injection Well Count	3	7
Scaling Potential	Undefined	Undefined
Non-Condensable Management	Required, not defined	In flash vessels
Heat for OTSG Replacement	383 MW	383 MW
Power Production	Additional potential for ORC with waste heat.	150 MW Power generation via turbine. Additional potential for ORC with waste heat.
Make-up Water Required	67 Ton/h	170 Ton/h
Surface Footprint	Lower	Higher

The non-flashing scenario operates with lower water consumption, lower well count, and a small footprint while providing the thermal energy to replace the OTSG. This option does offer both lower capital investment and operating costs.

The flashing case capitalizes on the thermal heat available providing the thermal energy to replace the OTSGs and generate a substantial amount of power but comes with both higher capital investment and operating costs. No plot plans were developed for either scenario. Plot areas were accounted for in the cost factors per the estimate basis, which utilizes the Class V methodology for capacity factoring, as guided by parametric models, judgment, or analogy.

Facility Capital Cost Estimate Basis

Project Description and Estimate Basis

The engineering details for this estimate are defined in the Estimate Basis attached in the Appendix.

Estimate Classification

The estimated costs are consistent with the development of a Class 5 estimate according to AACEI's RP's 18R-97 & 97R-18 with little engineering completed. A typical accuracy range for this type of project is in the range of +50% / - 30%, after application of an appropriate contingency. A formal risk analysis should be completed to assess contingency and determine the accuracy range.

Table 12: Class 5 estimate as defined by AACEi below (excerpt from RP 18R-97):

CLASS 5 ESTIMATE	
Description: Class 5 estimates are generally prepared based on very limited information, and subsequently have wide accuracy ranges. As such, some companies and organizations have elected to determine that due to the inherent inaccuracies, such estimates cannot be classified in a conventional and systematic manner. Class 5 estimates, due to the requirements of end use, may be prepared within a very limited amount of time and with little effort expended—sometimes requiring less than an hour to prepare. Often, little more than proposed plant type, location, and capacity are known at the time of estimate preparation. **Maturity Level of Project Definition Deliverables:** Key deliverable and target status: Block flow diagram agreed by key stakeholders. List of key design basis assumptions. 0% to 2% of full project definition. **End Usage:** Class 5 estimates are prepared for any number of strategic business planning purposes, such as but not limited to market studies, assessment of initial viability, evaluation of alternate schemes, project screening, project location studies, evaluation of resource needs and budgeting, long-range capital planning, etc.	**Estimating Methodology:** Class 5 estimates generally use stochastic estimating methods such as cost/capacity curves and factors, scale of operations factors, Lang factors, Hand factors, Chilton factors, Peters-Timmerhaus factors, Guthrie factors, and other parametric and modeling techniques. **Expected Accuracy Range:** Typical accuracy ranges for Class 5 estimates are -20% to -50% on the low side, and +30% to +100% on the high side, depending on the technological complexity of the project, appropriate reference information and other risks (after inclusion of an appropriate contingency determination). Ranges could exceed those shown if there are unusual risks. **Alternate Estimate Names, Terms, Expressions, Synonyms:** Ratio, ballpark, blue sky, seat-of-pants, ROM, idea study, prospect estimate, concession license estimate, guesstimate, rule-of-thumb.

Table 2a – Class 5 Estimate

Execution Strategy / Schedule

No details for execution or construction are yet contemplated. Costs derived generically without any specific strategy or timeline.

Cost Summary

The Total Cost in Q4 2022 CAD for the facilities and pipelines portion of the project are as follows:

1. Non-flashing scenario: $144,700,000 to $578,800,000 with a likely value centered on $289,387,000. Refer to Appendix.
2. Flashing scenario: $432,100,000 to $1,728,400,000 with a likely value centered on $864,207,000. Refer to Appendix.

Capital costs (including wells) for both scenarios are high to very high when compared to the existing source of heat for OTSGs. Major cost drivers are the very high pressures and temperatures at which the geothermal fluids are produced and injected, both above the critical point. These high pressures apply to surface pipelines and in-plant equipment. High volumes of geothermal water are required. However very large diameter pipe for 25 MPa

pressures, especially at up to 390°C may be difficult or impossible to procure. No field layout of wells was also created but a basic assumption that all wells are within 2 km of the CPF.

A great deal of uncertainty in the cost influence of the geothermal water quality on heat exchange and power equipment. While a generous allowance was made in this regard, it is unknow whether it will be sufficient to compensate.

Cost guidance for the heat exchange equipment and waste heat boilers was provided by THERMAL ENGINEERING INTERNATIONAL (USA) INC. A Babcock Power Inc. Company. Cost guidance for the power generation equipment was provided by Mitsubishi Heavy Industries (MHI).

VI. Economic Modelling

GLJ prepared a preliminary economic assessment for the Super Deep Geothermal Project in the Alberta Oil Sands to understand the high-level feasibility of the project. GLJ made use of the internal economic software with project specific modifications in Excel. Although several assumptions are required due to the high degree of uncertainty, GLJ considered the following factors when evaluating the economics:

Cost Inputs
- Capital
- Operating
- Maintenance
- Sustaining
- Decommissioning, Abandonment & Reclamation

Geothermal Production
- Electricity Generation
- Facility Design
- Well Capacity

Marketing
- Revenue from Power Sales
- Carbon Tax and Credits
- Oil Sands Royalties
- Pricing

Project Schedule
- Project Design
- Well Design and Drilling
- Construction
- Commissioning & Start-up

Summary of Scenarios

Ongoing OTSG
- 30,000 bbl/d of bitumen with and SOR = 3.0
- Currently producing at capacity after approximately 25 years of operation
- Assume the OTSGs will be replaced and in service by January 2030
- Major turnaround planned for a cost of $300 million
- Following the OTSG replacement, plant will continue for another 40 years
- Sustaining SAGD well pairs will be added as needed to keep the facility full

Greenfield OTSG
- 30,000 bbl/d of bitumen with and SOR = 3.0
- Brand new facility to be designed and constructed
- Project to start in 2023 and be ready for start-up in January 2030
- Total facility cost of $1,092 million
- Cost of initial SAGD well pairs is in addition to the facility
- Sustaining SAGD well pairs will be added as needed to keep the facility full for 40 years

Non-Flashing Geothermal – Low Well Cost / High Well Cost

- 30,000 bbl/d of bitumen with and SOR = 3.0
- Currently producing at capacity after approximately 25 years of operation
- Assume the OTSGs will be replaced with a geothermal system to generate 100% of the required steam by January 2030
- Geothermal facility is a non-flashing system described above, with less excess electricity available for sale
- Low Well Cost scenario assumes wells with good injection and production capacity, requiring less wells, and lower cost
- High Well cost scenario assumes more wells are required and higher well costs

Flashing Geothermal – Low Well Cost / High Well Cost

- 30,000 bbl/d of bitumen with and SOR = 3.0
- Currently producing at capacity after approximately 25 years of operation
- Assume the OTSGs will be replaced with a geothermal system to generate 100% of the required steam by January 2030
- Geothermal facility is a flashing system described above, with higher facility costs and significant electricity available for sale
- Low Well Cost scenario assumes wells with good injection and production capacity, requiring less wells, and lower cost
- High Well cost scenario assumes more wells are required and higher well costs

The cost of the base Greenfield SAGD facility was assumed using data GLJ has collected through years of experience evaluating the reserves and resources from most of the Alberta and Saskatchewan SAGD projects.

GLJ originally considered a scenario for a greenfield SAGD facility using geothermal technology. When reviewing the drilling and facility cost data it was determined that this is a highly unlikely and costly scenario. There have been very few discussions of a large-scale, greenfield SAGD facility from any of our clients. A super-major oil sands project would need to overcome many more environmental, political, and financial barriers than there were 20 years ago. In addition, the high-quality in-situ resources required to support a 30,000 bbl/d project are already being developed by the major oil sands companies with their currently operating facilities.

Economic Assumptions

Below is a summary of the key parameters in the economic model. Details on many of the technical parameters can be found in the previous sections. COSIA provided the SAGD facility design basis for the bitumen and steam capacities. This basis was used to find the geothermal heating requirements to generate sufficient steam to support a 30,000 bbl/d SAGD facility.

Table 13: Summary of Economic Assumptions

		Ongoing SAGD	Greenfield SAGD	Geothermal SAGD Non-Flashing		Geothermal SAGD Flashing	
				Low Well Count	High Well Count	Low Well Count	High Well Count
Bitumen Capacity	bbl/d	30,000					
Steam Capacity	bbl/d	90,000					
SOR		3.0					
Cumulative Production	mmbbls	446	395	445			
Bitumen Facility Cost	M$		270,000				
Steam Facility Cost	M$		810,000	289,000		864,000	
Infrastructure	M$		12,000	12,000		12,000	
ORC Power Generators	M$			80,000		160,000	
Total Facility Cost	M$		1,092,000	381,000		1,036,000	
Geothermal Injectors				3	6	7	14
Geothermal Producers				6	12	14	28
Injector Rate	bbl/d			50,000			
Producer Rate	bbl/d			25,000			
Geothermal Injector Well Cost	M$ each			100,000			
Geothermal Producer Well Cost	M$ each			90,000			
Total Geothermal Well Cost	M$			840,000	1,680,000	1,960,000	3,920,000
Ongoing Facility Turnaround	M$	300,000					
Annual Maintenance	M$	20,000					
Fixed Oil Operating Costs	$/bbl/bopd	625	625	350	350	350	350
Fixed Steam Operating Costs	$/bbl/bopd	625	625	200	200	200	200
Total Fixed Operaing Costs	M$/year	75,000	75,000	40,000	40,000	60,000	60,000
Variable Oil Costs	$/bopd	0.50	0.50	0.50	0.50	0.50	0.50
Variable Steam Costs	$/bspd	0.50	0.50	0.50	0.50	0.50	0.50
Power Offsales	MW			10		85	
SAGD Well Pair Drilling & Completion	M$ /well pair	4,500					
SAGD Well Pair Pad Equipment	M$ /well pair	3,500					
NPV10	MM$	2,481	782	2,245	1,718	1,527	299
NPV10/bbl	$/bbl	5.90	1.98	5.05	3.87	3.44	0.67

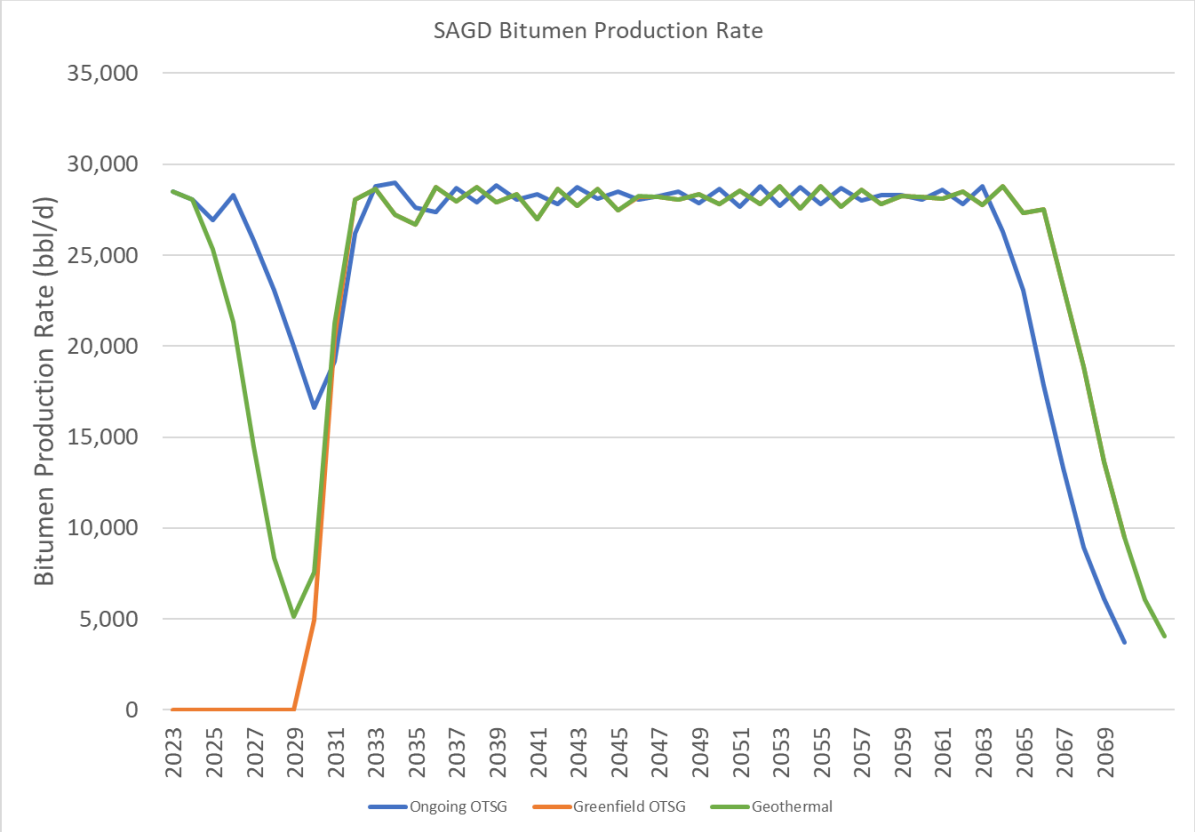

Figure 27: SAGD Bitumen Production Rates

Figure 27: SAGD Bitumen Production Rates compares the bitumen production rates for the scenarios. When comparing economic cases, it is important to have consistent timeframes and volumes. For this project, the Greenfield OTSG scenario produces less total bitumen because it only starts production in 2030. The Geothermal scenarios produce the same total volume as the Ongoing OTSG case, but because we have assumed a longer turnaround impact for the geothermal equipment, these scenarios produce a few years longer. Note how the production profiles for the Greenfield OTSG and all the Geothermal cases overlap after 2031.

Assumptions for the downtime profiles have been made by GLJ. The geothermal retrofit scenarios are assumed to require longer downtime than the OTSG replacement. These assumed durations are helpful to compare the overall economics of the scenarios and are within the accuracy of the estimates.

Carbon taxes have been included as operating costs considering historical carbon tax payments with price escalation from 2023 through 2030 in accordance with Canada's minimum national price on carbon pollution. Carbon pricing is modelled to increase to $170 /tonne by 2030. Although the legislation is very new, GLJ has included our interpretation of the SAGD benchmarks and the rules around tightening SOR limits. For simplicity, the geothermal scenarios assume zero carbon tax after 2030 since steam generated with these processes do not emit CO_2.

Economic Results

All the scenarios are economic with the assumptions described in this report.

Figure 28: NPV10 Cumulative Discounted Cash Flow displays the cumulative discounted cash flows for each of the scenarios, using a discount rate of 10%. The Non-Flashing Geothermal scenarios are economically competitive with the Ongoing SAGD scenario.

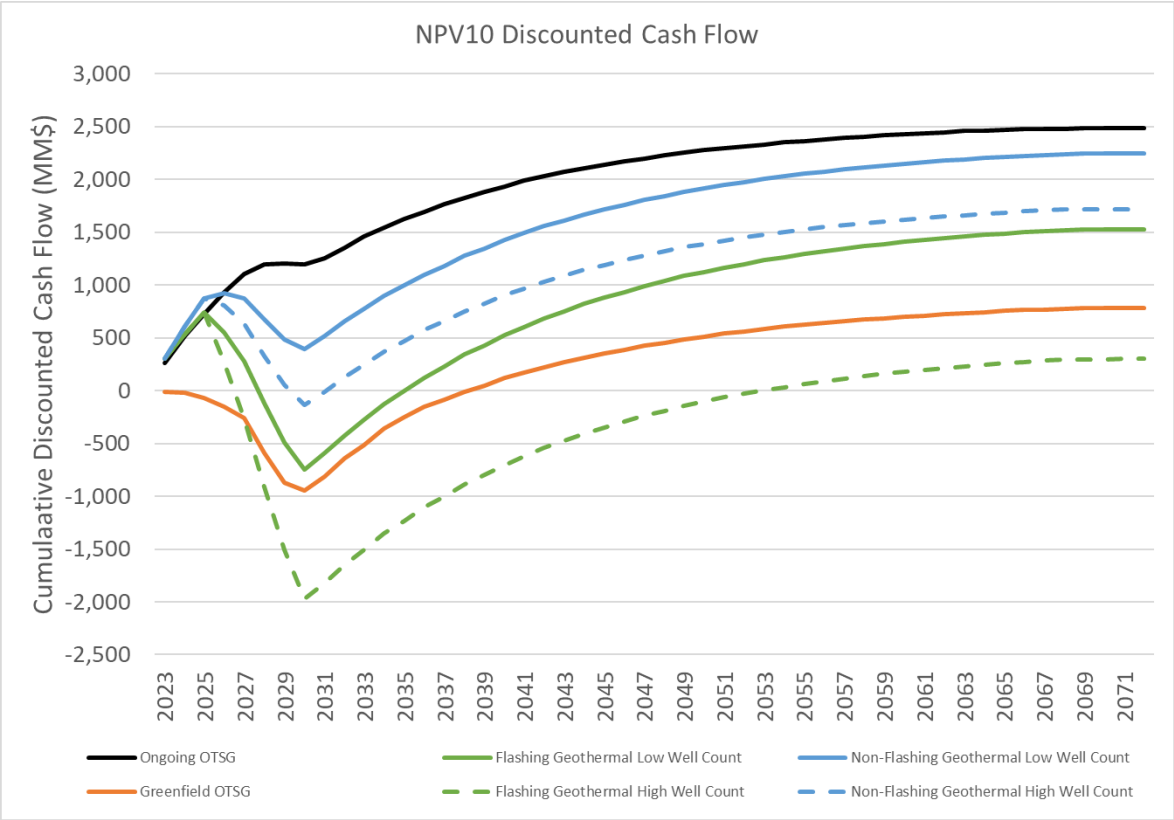

Figure 28: NPV10 Cumulative Discounted Cash Flow

Economic benefits of steam generated using a geothermal system include:

- Eliminate the cost of natural gas to generate steam
- Eliminate the rising carbon tax associated with burning natural gas
- Excess electricity generated by the process can be sold to provide baseload power to the grid
- Operating costs are lower than an OTSG facility

These economic benefits are clearly evident in Figure 29: Annual Inflated Cash Flow where the annual cash flows (undiscounted but inflated) for the geothermal scenarios are all higher than the OTSG scenarios.

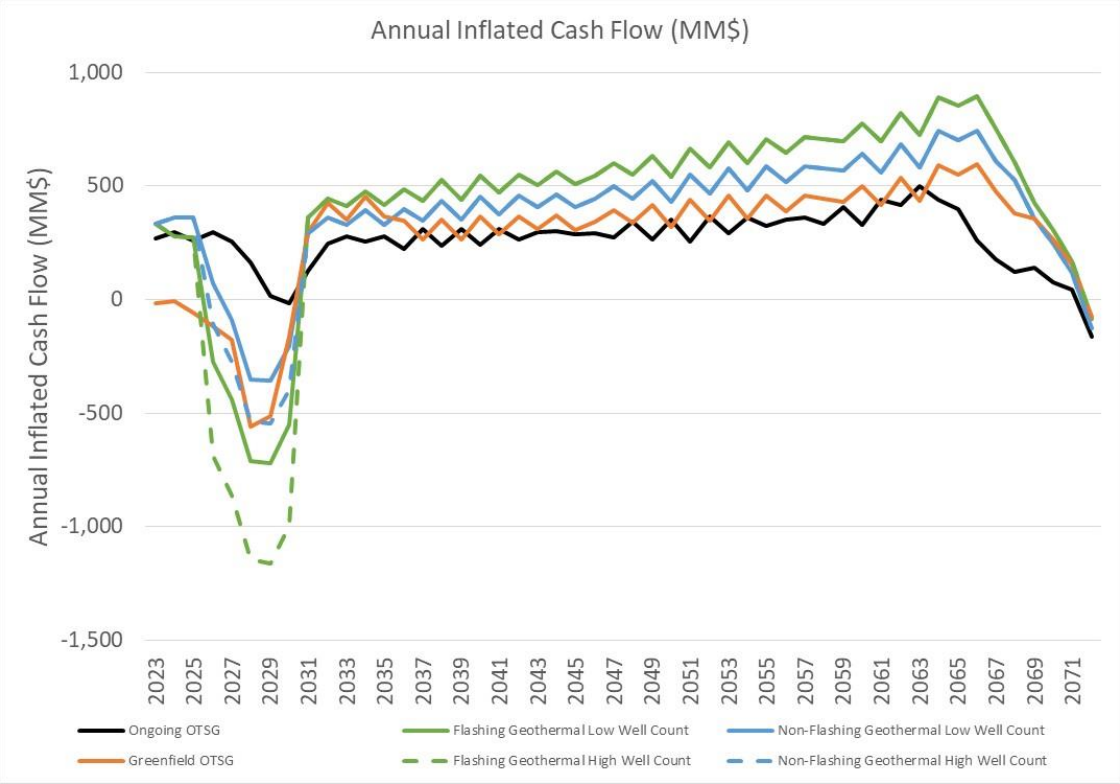

Figure 29: Annual Inflated Cash Flow

An overall comparison of the NPV10 for each of the scenarios is shown in Figure 30: Scenario NPV10 Comparison. The Non-Flashing scenarios are the most favourable of the geothermal cases investigated for this project, mainly due to the lower initial cost.

A fulsome probabilistic economic analysis outside the current scope of this project, however after working with the economic model, some obvious but key parameters can be identified.

- High degree of uncertainty in the facility cost estimates.
- Drilling cost estimates have a wide range of uncertainty along with the high degree of risk when drilling the wells.
- The injection and production flow potential of the geothermal reservoir has not been tested. This will impact the number of wells required and the cost of the project.

Using geothermal energy to generate steam for an established SAGD plant is more economically feasible than a stand-alone geothermal power facility. The economic benefit of being attached to a SAGD plant is the combination of revenue from both bitumen and power sales. The environmental benefits of geothermal also have a positive impact on the economics since the technology does not burn natural gas and avoids the growing carbon tax.

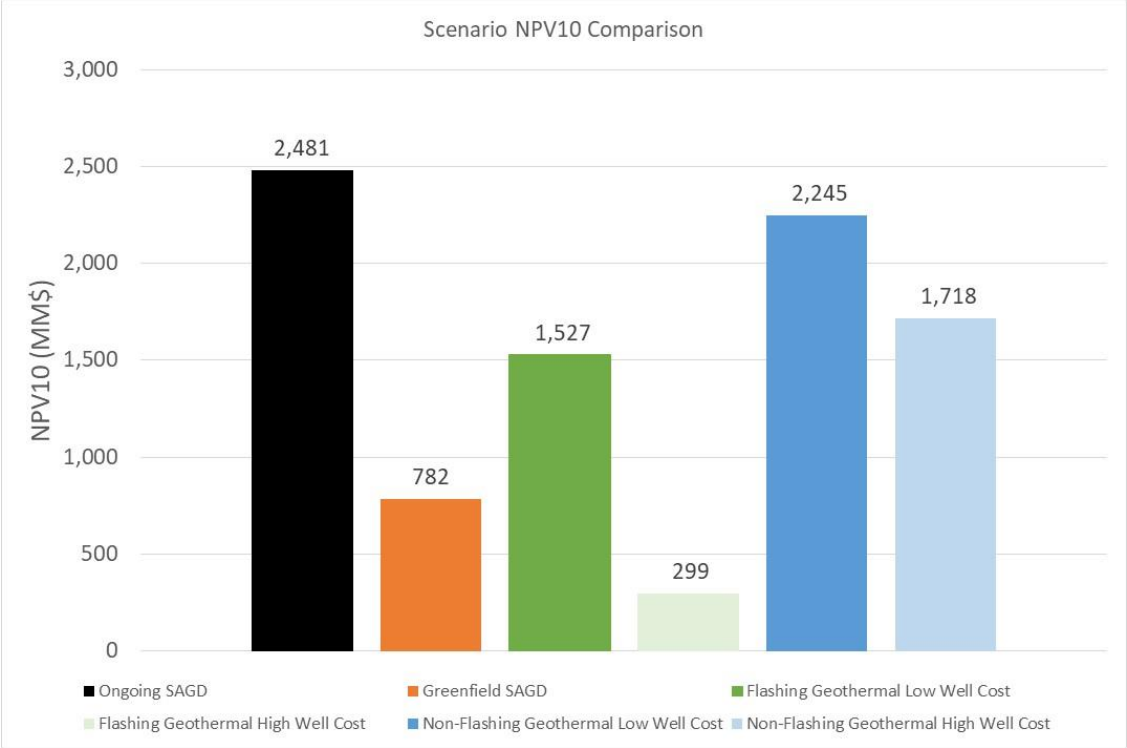

Figure 30: Scenario NPV10 Comparison

VII. Conclusions

This report provided a high-level review of the subsurface review including rock mechanics and fracability of the supercritical rock, geothermal resource and energy calculations, drilling, facilities, and an economic analysis. The key findings of these respective topics are included below:

- In the subsurface, the brittle-ductile transition due to high temperature is a key concept that controls the permeability, and therefore, exploitability of SHRs. Recent research shows rocks like granite can also remain brittle and frackable at their transition temperature and below it as well as research shows that pressures low as rock confining pressure are enough to stimulate a network of cloud fractures and create higher permeability in such resources.
- A geothermal resource certainly exists at depth if a fracture network and flow can be established between injector and producer wells. However, a considerable amount of drilling is required to access this resource to provide enough thermal energy to replace OTSGs.
- Drilling wells to access these resources will be a first of its kind. Over 15,000metres deep wells with 14,000metres through basement rock will be many firsts in the world in which would has many inherent risks. However, with advancements in drilling technologies such as development of better PDC drill bits there is a possibility for wells to be drilled faster than any ultra-deep wells previously. It is recommended before a full project is commissioned, that a pilot hole approximately 8,000 be drilled first to understand drilling speeds research quicker ways to drill through deep hot rock.
- Two technologies can be utilized to access the heat from the produced geothermal fluid, heat exchangers or a flash system. Due to the ultra-high temperatures and pressures both of these systems will be custom for this project. With the heat exchangers, less fluid is needed, however there is less additional electricity or mechanical energy which can be used from the geothermal fluid.
- The economics analysis shows that the non-flashing geothermal process to generate steam for a SAGD facility is the most feasible. With using geothermal there are cash flow benefits such as avoiding the cost of natural gas and the associated carbon tax. This process also provides power sales by installing an ORC generator on the hot water before it is reinjected.

Super Critical, or SHR Geothermal is a new geothermal technology that is in its infancy of being developed. There are associated risks and many unknowns with this project such as how wells will produce, drilling risks including drilling and completing the wells. However, based on this preliminary review many of these risks can be mitigated. Initial findings show that using geothermal in a SAGD project is economically feasible when analysing the project including SAGD well pairs and production. It is recommended that COSIA continues to investigate SHR and super critical geothermal and a path forward as it is an evolving technology which can assist with the production at SAGD facilities along with having a reduced environmental footprint on the path to net zero.

VIII. References

Acosta, M., Gibert, B., Violay, M., 2021, From Brittle to Ductile Deformation in the Continental Crust: Mechanics of Crystalline Reservoirs and Implications for Hydrothermal Circulation, Proceedings World Geothermal Congress 2020+1 Reykjavik, Iceland, April - October.

Ágústsson, K., Flóvenz, Ó.G., Guðmundsson, Á., Árnadóttir, S., 2012, Induced Seismicity in the Krafla High Temperature Field. GRC Transactions, 36, 2012, 975-980.

Bertani, R., Büsing, H., Buske, S., Dini, A., Hjelstuen, M., Luchini, M., Manzella, A., Nybo, R., Rabbel, W., Serniotti, L., 2018, the First results of the DESCRAMBLE Project. In: Proceedings, 43rd Workshop on Geothermal Reservoir Engineering, Stanford University, Stanford, California, February.

Brigham, W.E., Reed, P.W., Dew, J.N (1961) Experiments on Mixing During Miscible Displacement in Porous Media, SPE 1430-G.

Buijze, L., van Bijsterveldt, L., Cremer, H., Jaarsma, B., Paap, B., Veldkamp, H., Wassing, B., Jan-Diederik van Wees, J-D, van Yperen, G. , ter Heege, J., Induced Seismicity in Geothermal Systems: Occurrences Worldwide and Implications for the Netherlands, European Geothermal Congress 2019 Den Haag, The Netherlands, 11-14 June.

Danckwerts, P.V. (1953) Continuous Flow Systems. Distribution of Residence Times. Chemical Engineering Science, Volume 2, Issue 1, Pages 1-13.

Diez, H., Flores, M., Ramirez, M., Tovar, R., Rosales, C., Solano, F., Sandoval, F., 2015, Neutralization of Acid Fluids from Well H-43 (superheated steam), Los Humeros Geothermal Field, Mexico. In: Proceedings world geothermal congress 2015, Melbourne, Australia, 19–25 April.

Emmerman, R. Lauterjun, J., 1997, The Geramn Continental Deep Drilling Program KTB: Overview and major results, Journal of Geophysical Research, Bo.. 102, No B8, Pages 18,179-18,201.

Engvik, A. K., Bertram, A. , Kalthoff, J. F. , Stöckhert, B. , Austrheim, H. , Elvevold, S., 2005, Magma-driven Hydraulic Fracturing and Infiltration of Fluids into the Damaged Host Rock, an example from Dronning Maud Land, Antarctica, J. Struct. Geol., 27, 839–854.

Flóvenz, Ó.G., Ágústsson, K., Guðnason, E.Á., Kristjánsdóttir, S., 2015, Reinjection and Induced Seismicity in Geothermal Fields in Iceland, Proceedings World Geothermal Congress 2015 Melbourne, Australia, 19-25 April.

Friðleifsson, G.Ó., Elders, W.A., Zierenberg, R.A., Stefánsson A., Fowler, A.P.G., Weisenberger, T.B., Harðarson, B.S., Mesfn, K.G., 2017, The Iceland Deep Drilling Project 4.5 km deep well, IDDP-2, in the Sea-water Recharged Reykjanes geothermal field in SW Iceland Has Successfully Reached Its Supercritical Target. Sci Drill., 23:1–12.

Garrison, G.H., Uddenberg, M., Petty, S., Watz, J., Hill, B., 2020, Resource Potential of SuperHot Rock, GRC Transactions, Vol. 44.

Gaudreau, E., Audet, P. Schneider, D.A., 2019, Mapping Curie depth across western Canada from a wavelet analysis of magnetic anomaly data. Journal of Geophysical Research: Solid Earth, 124, 4365–4385. https://doi.org/10.1029/2018JB016726

Goto, R., Pramudyo, E., Miura, T., Watanabe, N., Sakaguchi, K., Komai, T., Tsuchiya, N., 2021, Hydraulic Fracturing and Permeability Enhancement in Granite at Supercritical Temperatures, Proceedings World Geothermal Congress 2020+1 Reykjavik, Iceland, April – October.

Ground Water Protection Council and Interstate Oil and Gas Compact Commission, 2021, Potential Induced Seismicity Guide: A Resource of Technical and Regulatory Considerations Associated with Fluid Injection, March, 250 pages.

Häring, M.O., Schanz, U., Ladner, F., Dyer, B. C., 2008, Characterisation of the Basel 1 Enhanced Geothermal System, Geothermics, 37, 469.
Hill, L.B., 2021, Superhot Rock Geothermal A Vision for Zero-Carbon Energy "Everywhere", Published by CATF (Clean Air Task Force), October.

Ingebritsen S.E., Manning, C.E., 1999 Geological Implications of a Permeability-depth Curve for the Continental Crust. Geology, 27, 1, 107–110.

Ingebritsen, S.E., Manning, C.E., 2010, Permeability of the Continental Crust: Dynamic Variations Inferred from Seismicity and Metamorphism, Geofluids, 10, 193–205.

Juncu, D., Árnadóttir, T., Geirsson, H., Guðmundsson, G. B., Lund, B., Gunnarsson, G., Michalczewska, K., 2018, Injection-induced Surface Deformation and Seismicity at the Hellisheidi Geothermal Field, Iceland, Journal of Volcanology and Geothermal Research.

Kaldal, G.S., Þorbjörnsson, O.I., 2016, Thermal Expansion of Casings in Geothermal Wells and Possible Mitigation of Resultant Axial Strain. In: European geothermal congress 2016, Strasbourg, France, 19–24 September.
Kim, K., Ree, J., Kim, Y., Kim, S., Kang, S. Y., Seo, W., 2018, Assessing Whether the 2017 Mw 5.4 Pohang earthquake in South Korea Was an Induced Event, Science, 360, 1007.

Kruszewski, M., Wittig, V., 2018, Review of Failure Modes in Supercritical Geothermal Drilling Projects, Geotherm Energy, 6:28.

Lavigne, J.; Maget, P. (1977) Les Ressources Géothermiques Française—Possibilités de Mise en Valeur; Report, 77 SGN 433 GTH; Bureau de Recherches Géologiques et Minières (BRGM): Orléans, France.

Lohman, R.B., McGuire, J.J., 2007, Earthquake swarms driven by aseismic creep in the Salton Trough, California, Journal of Geophysical Research, vol 112, B04405, doi:10.1029/2006JB004596.

Okada, T., Matsuzawa, T., Umino, N., Yoshida, K. , Hasegawa, A. , Takahashi, H. , Yamada, T. , Kosuga, M. Takeda, T., Kato, A., Igarashi, T., Obara, K., Sakai, S., Saiga, A., Iidaka, T., Iwasaki, T., Hirata, N., Tsumura, N., Yamanaka, Y., Terakawa, T., Nakamichi, H., Okuda, T., Horikawa, S., Katao, H., Miura, T., Kubo, A., Matsushima, T., Goto, K., Miyamachi, H., 2015, Hypocenter Migration and Crustal Seismic Velocity Distribution Observed for the Inland Earthquake Swarms Induced by the 2011 Tohoku-Oki Earthquake in NE Japan: Implications for Crustal Fluid Distribution and Crustal Permeability, Geofluids, 15, 293–309.

Majer, E. L., Freeman, K., Johnson, L., Jarpe, S., Nihei, K. T., Hartline, C., Walter, M., Deniliger, M., 2017, Monitoring the Effect of Injection of Fluids from the Lake County Pipeline on Seismicity at The Geysers, California, Geothermal Field, Final Report, Lawrence Berkeley National Laboratory, Calpine Corporation, Lake County.

Petty, S., Watz, J., Garrison, G., 2020, Technology Needs for SuperHot EGS Development, PROCEEDINGS, 45th Workshop on Geothermal Reservoir Engineering Stanford University, Stanford, California, February 10-12.

Þorbjörnsson, O.I., Karlsdottir, N.S., Einarsson, A., Ragnarsdottir, R.K., 2015, Materials for Geothermal Steam Utilization at Higher Temperatures and Pressures. In: Proceedings World Geothermal Congress 2015, Melbourne, Australia, 19–25 April.

Ramey H. J. (1962) Wellbore Heat Transmission, SPE 96, April 1962

Reinsch, T., Dobson, P.Asanuma, H., Huenges, E., Poletto, F., Sanjuan, B., 2017, Utilizing Supercritical Geothermal Systems: A Review of Past Ventures and Ongoing, Reinsch et al. Geotherm Energy, 5:16.

Scholz, C.H., 2019, The Mechanics of Earthquakes and Faulting, Third Edition, Cambridge University Press.
Scott, S., Driensner, T., Weis, P., 2015, Geologic Controls on Supercritical Geothermal Resources above Magmatic Intrusions, Nature Communications, DOI: 10.1038/ncomms8837.

Suzuki, Y., Ioka, S., Muraoka, H., 2014, Determining the Maximum Depth of Hydrothermal Circulation Using Geothermal Mapping and Seismicity to Delineate the Depth to Brittle-Plastic Transition in Northern Honshu, Japan, Energies, 7, 3503-3511; doi:10.3390/en7053503.

Teodoriu, C., 2015, Why and When Does Casing Fail in Geothermal Wells: a Surprising Question? In: Proceedings world geothermal congress 2015, Melbourne, Australia, 19–25 April.

Tsuchiya, N., 2017, Potential Candidates of Supercritical Geothermal Reservoir, GRC Transactions, Vol. 41.
Watanabe, N. Egawa, M., Sakaguchi, K., Ishibashi, T., Tsuchiya, N., 2017, Hydraulic Fracturing and Permeability Enhancement in Granite from Subcritical/Brittle to Supercritical/Ductile Conditions, Geophysical Research Letters, May, DOI: 10.1002/2017GL073898.

Watanabe N., Sakaguchi, K., Goto,R., Miura, T., Yamane, K., Ishibashi, T., Chen, Y. Komai, T, and Tsuchiya, N., 2018, Cloud-fracture Networks as a Means of Accessing Superhot Geothermal Energy, Scientific Reports, 9:939.

White D.E. & Williams D.L, (1974), Assessment of Geothermal Resources of the United States, Circular 726, USGS

Williams, C.F., (2007). Updated methods for estimating recovery factors for geothermal resources. In: Proceedings, Thirty-Second Workshop on Geothermal Reservoir Engineering. Stanford University, January 22–24, 2007, SGP-TR-183. 7 p.

IX. APPENDIX

A. Non-Flashing Block Flow Diagram

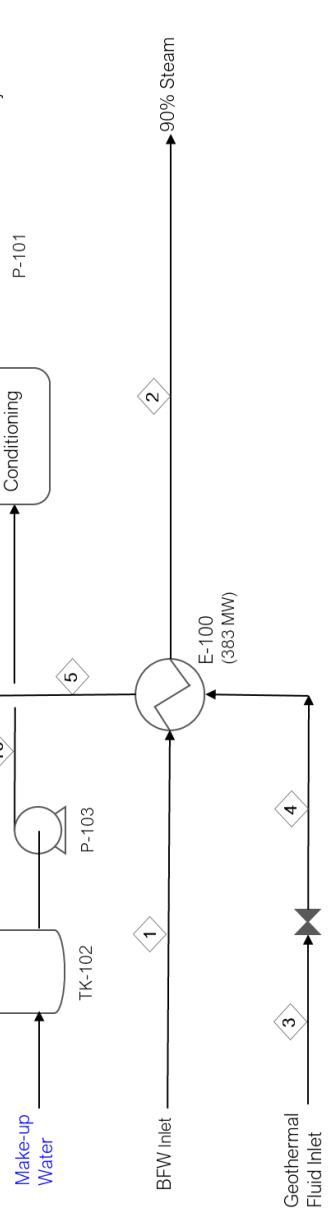

Stream Number		1	2	3	4	5	6	7	8	9	10
Stream Description		BFW Inlet	Heated BFW	Geothermal Fluid @ Reservoir Cond.	Geothermal Fluid @ Surface Cond.	Cooled Geothermal Fluid	Geothermal Fluid to Conditioning	Conditioned Geothermal Fluid	Geothermal Fluid for Reinjection	5% Geothermal Fluid to Disposal	Make-up Water
Volumetric Flow Rate	m^3/h	800	12,100	1,917	2,498	1,474	1,400	1,461	1,460	74	66
Mass Flow Rate	kg/h	727,945	727,945	1,336,270	1,336,270	1,336,270	1,269,460	1,336,270	1,336,270	66,810	66,810
Temperature	°C	163	310	400	365	173	173	165	16	173	7
Pressure	MPa	10.4	9.9	150	22	21.5	21.5	21.5	25	21.5	21.5
Vapour Fraction	-	0	0.9	0	0	0	0	0	0	0	0

B. Flashing Block Flow Diagram

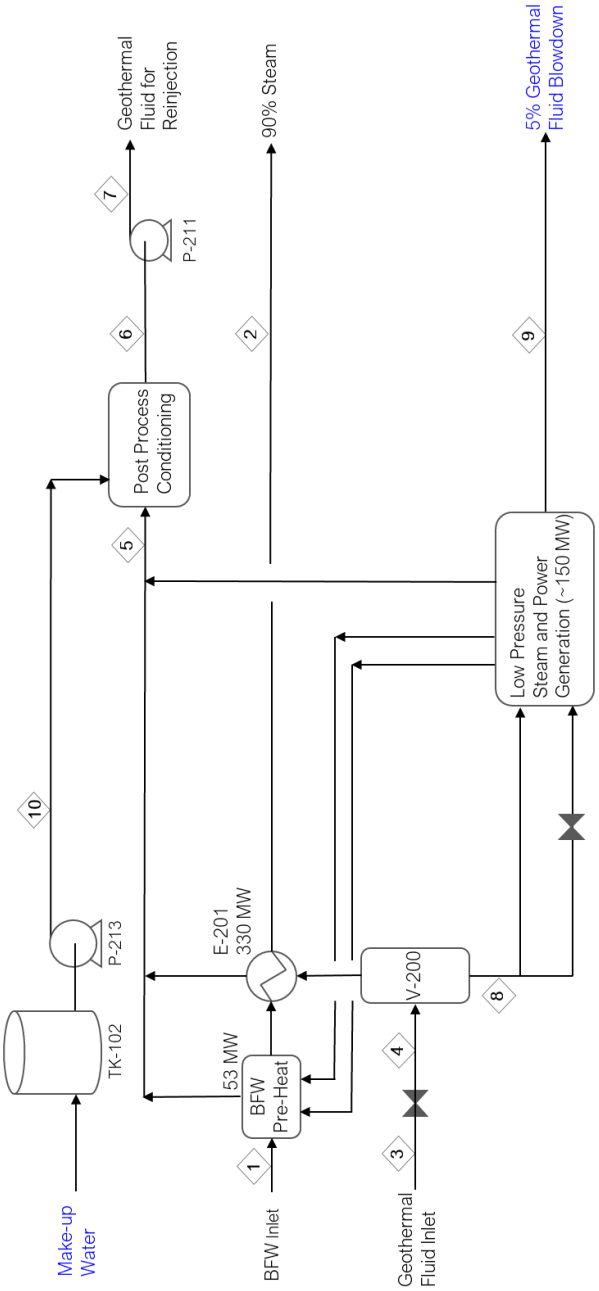

Stream Number		1	2	3	4	5	6	7	8	9	10
Stream Description		BFW Inlet	Heated BFW	Geothermal Fluid @ Reservoir Cond.	Geothermal Fluid @ Surface Cond.	Geothermal Fluid to Conditioning	Conditioned Geothermal Fluid	Geothermal Fluid for Reinjection	HP Flash Separator Liquids	5% Geothermal Fluid to Disposal	Make-up Water
Volumetric Flow Rate	m^3/h	800	12,100	4,877	12,988	3,677	3,827	3806	4,254	175	169
Mass Flow Rate	kg/h	727,945	727,945	3,398,400	3,398,400	3,229,200	3,398,400	3,398,400	2,689,200	170,000	170,000
Temperature	°C	163	310	400	333	195	186	189	333	90	6
Pressure	MPa	10.4	9.9	150	13.4	12.9	12.9	25	13.4	13	13
Vapour Fraction	-	0	0.9	0	0.21	0	0	0	0	0	0

Geothermal SAGD

Class 5
COST ESTIMATE BASIS

C	2022-11-27	Issued for Review (Updated pricing and design info)	PG		
B	2022-11-21	Issued for Review	PG	GB	
A	2022-11-21	Issued for Review	PG	GB	
Rev.	**Date**		**By**	**Reviewed**	**Approved**

TABLE OF CONTENTS

1. PURPOSE

COSIA is looking for ways to reduce energy use and associated GHG emissions through the development of innovative technologies for SAGD plants. One such technology is using Geothermal Wells to generate steam and produce power. A class 5 estimate is required to better understand the economics of such a project.

The following sections describe the methodology for the basis of estimate.

2. PROJECT DESCRIPTION

The Geothermal SAGD facility is based on CPF#2 of the six reference CPF's identified and detailed in Candor Engineering's Project Report dated August 16, 2018. This SAGD facility will use mechanical lift to produce emulsion from the reservoir and evaporators for water treatment. For steam generation, the OTSG's from the reference facility will be replaced with Geothermal Wells. Only the Geothermal portion of the facility is estimated and based on the following two options:

- Option 1 – Non-Flashing – Geothermal wells used for generation of steam to insert into the reservoir only
- Option 2 – Flashing – Geothermal wells used for generation of steam to insert into the reservoir and to generate power that can be used at the facility and return excess to the grid

2.1 ESTIMATE CLASSIFICATION AND ACCURACY

Engineering

Engineering is in the very early stages of definition and so the estimate accuracy is Class 5 (+100% / -50%) according to AACE's Cost Estimate Classification Matrix (see table below).

Methodology

Although minimal engineering has been completed, the estimate for the steam generation portion of the plant will be developed using equipment factors for direct costs as there are no capacity factors that this technology can be scaled from. Indirect and other project costs will be generated by applying typical percentages against the direct costs.

The balance of plant will be estimated using historical SAGD benchmarks.

COST ESTIMATE CLASSIFICATION MATRIX FOR THE PROCESS INDUSTRIES

	Primary Characteristic	*Secondary Characteristic*		
ESTIMATE CLASS	**MATURITY LEVEL OF PROJECT DEFINITION DELIVERABLES** Expressed as % of complete definition	**END USAGE** Typical purpose of estimate	**METHODOLOGY** Typical estimating method	**EXPECTED ACCURACY RANGE** Typical variation in low and high ranges [a]
Class 5	0% to 2%	Concept screening	Capacity factored, parametric models, judgment, or analogy	L: -20% to -50% H: +30% to +100%
Class 4	1% to 15%	Study or feasibility	Equipment factored or parametric models	L: -15% to -30% H: +20% to +50%

	Primary Characteristic	*Secondary Characteristic*		
ESTIMATE CLASS	**MATURITY LEVEL OF PROJECT DEFINITION DELIVERABLES** Expressed as % of complete definition	**END USAGE** Typical purpose of estimate	**METHODOLOGY** Typical estimating method	**EXPECTED ACCURACY RANGE** Typical variation in low and high ranges [a]
Class 3	10% to 40%	Budget authorization or control	Semi-detailed unit costs with assembly level line items	L: -10% to -20% H: +10% to +30%
Class 2	30% to 75%	Control or bid/tender	Detailed unit cost with forced detailed take-off	L: -5% to -15% H: +5% to +20%
Class 1	65% to 100%	Check estimate or bid/tender	Detailed unit cost with detailed take-off	L: -3% to -10% H: +3% to +15%

Notes: [a] The state of process technology, availability of applicable reference cost data, and many other risks affect the range markedly.
The +/- value represents typical percentage variation of actual costs from the cost estimate after application of contingency
(Typically at a 50% level of confidence) for given scope.

2.2 CONTROLLING DOCUMENTATION

This Class 5 estimate is based on the following documents:

- Mechanical Equipment List

2.3 WORK BREAKDOWN STRUCTURE

No project-specific WBS is used. Costs are summarized into a Level 1 Summary.

2.4 EXECUTION STRATEGY / SCHEDULE

A project execution strategy was not provided. It is unknown where or when construction will occur.

2.5 CONTRACTING / RESOURCE STRATEGY

A contracting strategy was not provided. It is unknown how the work will be contracted.

3. COST BASIS

3.1 Cost Summary

The Total Installed Cost (TIC) for each option is based on 4th Quarter 2022 CDN Dollars and shown below **including recommended contingency**:

Description	Costs - $MM CDN
Option 1 – Non-Flashing	$289.4
Option 2 – Flashing	$864.2

3.2 Scope / Assumptions

The following key assumptions are used to generate the Class 5 estimate for each option:

1) Option 1 – Non-Flashing
    a. Reference facility costs not included
    b. New Geothermal Steam Generation design will fit in the same location as the previous OTSG design with no changes to the reference facility (ie. central piperack, power distribution, control room and infrastructure) except for:
        i. An allowance to expand the plot space for the make up water treatment
        ii. The new Geothermal Steam Generation design will require an addition to the existing Steam Generation MCC
        iii. 12 Geothermal Wells are required approximately 2km from the plant, each running independently to the plant in 8" sch 160 pipelines – above grade lines
        iv. 6 Injection Wells are required approximately 2km from the plant, each running independently from the plant in 10" sch 160 pipelines – above grade lines
2) Option 2 – Flashing
    a. Reference facility costs not included
    b. New Geothermal Steam Generation design will fit in the same location as the previous OTSG design with no changes to the reference facility (ie. central piperack, power distribution, control room and infrastructure) except for:
        i. An allowance to expand the plot space for the make up water treatment and power generation
        ii. The new Geothermal Steam Generation design will require an addition to the existing Steam Generation MCC
        iii. 29 Geothermal Wells are required approximately 2km from the plant, each running independently to the plant in 8" sch 160 pipelines – above grade lines
        iv. 14 Injection Wells are required approximately 2km from the plant, each running independently from the plant in 10" sch 160 pipelines – above grade lines
        v. 4 Blowdown wells are required approximately 5km from the plant, each running independently from the plant in 6" pipelines – above grade lines
        vi. It is assumed the power feed and connection to the grid from the Power Generation unit can be done for same price as the distribution included in the reference facility

3.3 Equipment & Module Pricing

Equipment pricing is budgetary from specialized vendors where possible, otherwise scaled from historical pricing. Module pricing is from recent historical projects.

3.4 Material & Subcontractor Pricing

Bulk material and subcontractor pricing is from recent historical projects.

3.5 Labour

Labour installation rates are from recent historical projects. They are based on greenfield conditions and include productivity adjustments for the location, complexity of project and weather.

The average labour rate used for direct field work and manual indirect field work is $75.00 per hour. This rate is consistent with CLAC rates on 10 hour days, a 10 day on / 4 day off shift and a majority Journeyman crew mix.

3.6 Design / MTO Allowances

Design and MTO allowances are not required as the module costs and key quantities are expected to be inclusive of these allowances.

3.7 Freight

An allowance of 5% is applied on equipment and material pricing to account for freight unless included in the equipment pricing itself

3.8 Scaffolding

An allowance of 18% on all field hours is carried for scaffolding.

3.9 Construction Indirects

Indirect costs are based on the use of a general contractor. The following percentages are used:

- Construction Services – 40% of Direct Field Labour Cost
- Construction Field Staff – 30% of Direct Field Labour Cost
- Temporary Construction Facilities – 15% of Direct Field Labour Cost
- Construction Equipment – 25% of Direct Field Labour Cost
- Overheads & Fees – 10% of Direct Field Labour Cost

3.10 Engineering Services

Engineering costs, inclusive of FEED, Detailed Engineering and 3rd Party support, are calculated using a percentage of 12% on Total Construction Costs.

3.11 Other Project Costs

Other project costs are calculated using the following percentages:

- Start Up & Commissioning – 3% of Total Installed Cost
- Owner's Cost – 3% of Total Installed Cost

3.12 Contingency

A contingency of 25% on all project costs is used for the purpose of this estimate. The contingency is used to cover the uncertainties and unforeseeable elements typical at the current level of scope definition. The contingency is applied to the new Geothermal SAGD items only as the historical SAGD benchmarks are inclusive.

3.13 Currency & Exchange Rates

All costs are in Canadian Dollars. Only the Steam Turbine in Option 2 – Flashing was sourced outside of Canada.

3.14 Forward Escalation

No escalation has been applied to the estimate. It should be noted that escalation in 2021 and 2022 has been higher than normal at ~ 9% and 5%, respectively.

3.15 Exclusions

The following costs have been excluded:

- Drilling
- Purchase or installation of the ESPs

4. RISKS

- A risk assessment was not performed on this estimate.
- The same economic environment may not exist at time of build.

5. ATTACHMENTS

- Estimate Summaries

cosia CANADA'S OIL SANDS INNOVATION ALLIANCE	Class 5 - Study Cost Estimate -50 / +100 %	
	COSIA	Revision: C
	Geothermal SAGD - Non-Flashing	Date: November 27, 2022
	Location Unknown	PM/PE: GLJ
	Study	Estimator: Paul Goolcharan

Estimate Summary - Geothermal SAGD - Non-Flashing

DIRECT COSTS

Factored Costs		Cost	
Process Equipment & Modules	$	34,290,000	Steam Generation Unit Only
Freight	$	5,013,000	
Labour	$	7,003,200	
Bulk Material	$	10,504,800	
Total Factored Costs	$	56,811,000	
Non-Factored Costs			
Earthwork	$	2,500,000	Increased plot space for Make-Up Water
Civil, Structural & Architectural	$	-	
Piping	$	120,000,000	Pipelines
Electrical & Instrumentation	$	2,288,750	Steam Generation MCC & Homeruns
Demolition	$	-	
Total Non-Factored Costs	$	124,788,750	
Total Direct Cost	**$**	**181,599,750**	

INDIRECT COSTS

Contractor's Indirect Field Costs			**Basis**
Construction Services	$	2,832,780	40% of Direct Labour cost (40/60 L & M splits)
Field Staff	$	2,124,585	30% of Direct Labour cost
Temporary Facilities	$	1,062,293	15% of Direct Labour cost (40/60 L & M splits)
Construction Equipment	$	1,770,488	25% of Direct Labour cost (40/60 L & M splits)
Overheads & Fee	$	708,195	10% of Direct Labour cost (40/60 L & M splits)
Major Subcontract Allowance	$	-	0% of Major S/C costs
Scaffolding	$	1,274,751	18% of Direct Labour cost (above foundations)
On-Site Material Handling	$	-	0% of Materials & Equipmenct cost
Camp/Subsistence Costs (DFL + S/C + Ind. Hrs.)	$	2,905,305	$ 20.00 man hours (direct & Ind. DFH)
Travel & Bussing (Origin to Camp to site & vise versa)	$	726,326	$ 5.00 per man hour (direct & Indirect)
Total Indirect Costs	**$**	**13,404,722**	
Engineering & Planning	$	23,400,537	12% of Total Field Costs

TOTAL INSTALLED COST	$	218,405,009	Total of Direct & Indirect Construction Costs
Commissioning & Start-Up	$	6,552,150	3% of Total Installed Cost
Owner's Construction Management	$	-	0% of Total Installed Cost
Owners Cost	$	6,552,150	3% of Total Installed Cost
Contingency	$	57,877,327	25% of TIC and Owners Costs
TOTAL PROJECT COST	$	289,387,000	CDN
Low Range -50%	$	144,700,000	
High Range +100%	$	578,800,000	

Class 5 - Study Cost Estimate
-50 / +100 %

COSIA | Revision: C
Geothermal SAGD - Flashing | Date: November 27, 2022
Location Unknown | PM/PE: GLJ
Study | Estimator: Paul Goolcharan

Estimate Summary - Geothermal SAGD - Flashing

DIRECT COSTS

Factored Costs		Cost	
Process Equipment & Modules	$	110,100,000	Steam Generation Unit Only
Freight	$	7,660,720	
Labour	$	43,904,000	
Bulk Material	$	65,856,000	
Total Factored Costs	$	227,520,720	
Non-Factored Costs			
Earthwork	$	5,000,000	Increased plot space for Make-Up Water
Civil, Structural & Architectural	$	-	
Piping	$	261,600,000	Pipelines
Electrical & Instrumentation	$	5,787,500	Steam Generation MCC & Homeruns
Demolition	$	-	
Total Non-Factored Costs	$	272,387,500	
Total Direct Cost	**$**	**499,908,220**	

INDIRECT COSTS

Contractor's Indirect Field Costs			Basis
Construction Services	$	17,645,600	40% of Direct Labour cost (40/60 L & M splits)
Field Staff	$	13,234,200	30% of Direct Labour cost
Temporary Facilities	$	6,617,100	15% of Direct Labour cost (40/60 L & M splits)
Construction Equipment	$	11,028,500	25% of Direct Labour cost (40/60 L & M splits)
Overheads & Fee	$	4,411,400	10% of Direct Labour cost (40/60 L & M splits)
Major Subcontract Allowance	$	-	0% of Major S/C costs
Scaffolding	$	7,940,520	18% of Direct Labour cost (above foundations)
On-Site Material Handling	$	-	0% of Materials & Equipmenct cost
Camp/Subsistence Costs (DFL + S/C + Ind. Hrs.)	$	17,251,548	$ 20.00 man hours (direct & Ind. DFH)
Travel & Bussing (Origin to Camp to site & vise versa)	$	4,312,887	$ 5.00 per man hour (direct & Indirect)
Total Indirect Costs	**$**	**82,441,755**	
Engineering & Planning	$	69,881,997	12% of Total Field Costs

TOTAL INSTALLED COST	$	652,231,972	Total of Direct & Indirect Construction Costs
Commissioning & Start-Up	$	19,566,959	3% of Total Installed Cost
Owner's Construction Management	$	-	0% of Total Installed Cost
Owners Cost	$	19,566,959	3% of Total Installed Cost
Contingency	$	172,841,473	25% of TIC and Owners Costs
TOTAL PROJECT COST	$	864,207,000	CDN
Low Range -50%	**$**	**432,100,000**	
High Range +100%	**$**	**1,728,400,000**	